MASTER EN BIOCHIMIE ET BIOLOGIE MOLÉCULAIRE ET CELLULAIRE

In vivo characterization of Bruce/la melitensis growth in lung alveolar macrophages of intranasally infected mice

Lagneaux, Maxime

Award date:
2017

Awarding institution:
Universite de Namur

Faculté des Sciences

IN VIVO CHARACTERIZATION OF *BRUCELLA MELITENSIS* GROWTH IN LUNG ALVEOLAR MACROPHAGES OF INTRANASALLY INFECTED MICE

Mémoire présenté pour l'obtention

du grade académique de master 120 en biochimie et biologie moléculaire et cellulaire

Maxime LAGNEAUX

Janvier 2017

Université de Namur
FACULTE DES SCIENCES
Secrétariat du Département de Biologie
Rue de Bruxelles 61 - 5000 NAMUR
Téléphone: + 32(0)81.72.44.18 - Téléfax: + 32(0)81.72.44.20
E-mail: joelle.jonet@unamur.be - http://www.unamur.be

In vivo characterization of *Brucella melitensis* growth in lung alveolar macrophages of intranasally infected mice

LAGNEAUX Maxime

Summary

Brucella spp. are facultative intracellular bacteria responsible for brucellosis, a chronic zoonotic disease which cause abortion in infected cattle. Brucellosis is transmitted to humans through the consumption of infected animal products or aerosols. There are currently no safe or efficient vaccine, and the treatment involves long term antibiotics uptake.

Following intranasal infection, *Brucella melitensis* infects primarily alveolar macrophages and persists in the lungs for a few days before being progressively cleared out and disseminating through the organism. Previous studies showed that the control of *Brucella* in the lungs involves T_H17 mediated responses at 5 days post infection, and T_H1 mediated responses in later times. In the chronic phase of infection, *Brucella* settles in the spleen, sheltered from the immune response. That is why the control of *Brucella* infection is crucial during its early stages.

Our objectives were to characterize the early times of infection (0-48 hours) *in vivo* following intranasal inoculation of *Brucella melitensis* in mice models. We used three strategies to address this problem : confirming by flow cytometry the phenotype of the lungs infected cells in early times of infection, visualizing *Brucella* growth and division *in vivo* by microscopy, and identifying a role of the immune response in the control of the infection by comparing the resistance of various mice deficient for key elements of the immune system.

During this study, we used eFluor 670 to label the membrane of the bacteria. This allowed us to formally identify by flow cytometry the *Brucella*-infected cells as alveolar macrophages. This staining also helped us to discriminate mother cells from daughter cells *in vivo* by microscopy. Finally, we demonstrated that T cells were implicated in the early control of intranasal *Brucella* infection, and that allergic asthma favors *Brucella* growth in the lungs.

Master 120 Thesis in Molecular and Cellular Biochemistry and Biology

January 2017

Promotor: Eric MURAILLE **Co-Promotors:** Jean-Jacques LETESSON / Xavier DE BOLLE

Université de Namur
FACULTE DES SCIENCES
Secrétariat du Département de Biologie
Rue de Bruxelles 61 - 5000 NAMUR
Téléphone: + 32(0)81.72.44.18 - Téléfax: + 32(0)81.72.44.20
E-mail: joelle.jonet@unamur.be - http://www.unamur.be

Caractérisation de la croissance de *Brucella melitensis in vivo* dans les macrophages alvéolaires du poumon de souris après infection intranasale

LAGNEAUX Maxime

Résumé

Les *Brucella* spp. sont des bactéries intracellulaires facultatives responsables de la brucellose, une zoonose chronique provoquant l'avortement chez le bétail infecté. La brucellose est transmise à l'homme via la consommation de produits animaux infectés ou par aérosols. Il n'y a actuellement aucun vaccin sûr ou efficace, et le traitement antibiotique est long et coûteux.
Après une infection intranasale, *Brucella melitensis* infecte d'abord les macrophages alvéolaires et persiste dans le poumon pendant quelques jours avant d'en être éliminée et de disséminer dans l'organisme. Des études ont montré que le contrôle de *Brucella* dans les poumons implique une réponse T_H17 à 5 jours post infection, suivie d'une réponse T_H1. Durant sa phase chronique, *Brucella* s'établit dans la rate, et y semble protégée de la réponse immunitaire. C'est pourquoi un contrôle de l'infection par *Brucella* durant les premières étapes de l'infection est essentiel.
Nos objectifs étaient de caractériser *in vivo* les temps précoces (0-48 heures) de l'infection intranasale par *B. melitensis* dans le modèle murin. Nous avons utilisé trois stratégies pour aborder cette question: confirmer formellement le phénotype des cellules infectées du poumon par cytométrie de flux, visualiser en microscopie la croissance et la division de *Brucella in situ*, et déterminer si le système immunitaire contrôle les premières étapes de l'infection.
Durant cette étude, nous avons utilisé l'eFluor 670 pour marquer les membranes bactériennes. Cet outil nous a permis d'identifier par cytométrie de flux les cellules infectées après infection intranasale comme étant des macrophages alvéolaires. Il nous a également permis de distinguer les bactéries mères des bactéries filles *in situ* par microscopie. Enfin, nous avons pu mettre en évidence un rôle des lymphocytes T dans le contrôle précoce de l'infection ainsi qu'une augmentation de la croissance bactérienne dans le poumon de souris sensibilisées à l'asthme.

Mémoire de master 120 en biochimie et biologie moléculaire et cellulaire
Janvier 2017
Promoteur: Eric MURAILLE **Co-Promoteurs:** Jean-Jacques LETESSON / Xavier DE BOLLE

Remerciements

Cette année aura été riche en émotions et en épreuves, et lorsque je relis le premier manuscrit du début d'année, ainsi que la première ébauche de remerciements que j'avais réalisée au même moment, je me rends compte à quel point l'évolution a été rapide tant sur le plan relationnel que professionnel. C'est avec le premier recul que j'ai maintenant que je vais pouvoir dédicacer ce travail aux gens qui ont fait de ce mémoire une belle aventure.

Je remercie avant tout mon promoteur Monsieur Eric Muraille pour sa patience, sa gentillesse, sa compréhension et sa disponibilité. Vous avez toujours fait en sorte de nous mettre à l'aise et de nous permettre de garder plaisir à faire de la recherche sans nous enfermer dans la monotonie et les horaires de bureau. Merci également pour m'avoir aidé sur le plan relationnel lorsque cela n'allait pas et m'avoir fait grandir.

Je remercie également mes co-promoteurs, le Professeur Jean-Jaques Letesson, pour sa gentillesse et ses nombreux conseils, et pour avoir veillé sur Margaux et moi depuis la première prise de sang jusqu'à l'écriture de ce mémoire, et le Professeur Xavier De Bolle pour sa bonne humeur et son écoute.

Je remercie Georges pour m'avoir aiguillé avant de me laisser prendre mon indépendance. Je sais à quel point cette année n'a pas été facile pour toi et que je n'étais peut-être pas le caractère idéal pour ta première fois en tant qu'encadrant, mais je pense que l'essentiel de ton travail était de me donner l'occasion de faire mes preuves par moi-même, et tu l'as fait.

Je remercie également Arnaud Machelart pour m'avoir pris sous son aile et soutenu pendant la première partie de l'année, pour ses conseils et sa bonne humeur, ainsi que Kevin et Katy pour m'avoir aidé et accompagné dans ma découverte de l'*in vitro*.

Dunia, Emeline et Katy, je ne vous remercierai jamais assez pour toute la gentillesse et la sympathie que vous m'avez témoignées, pour m'avoir donné le sourire à chaque fois que je vous croisais et pour m'avoir fait découvrir le Mojito-Fraise-Mais-Avec-Du-Rhum-Brun-SVP. Je vous tiens responsable pour tout ceux que j'ai bu par la suite.

Je remercie Jérôme, Séverin, Kenny et Régis pour leur bonne humeur et pour m'avoir accueilli dans leur Caulo-sanctuaire en fin d'année.

Merci à Estelle pour nous avoir donné le Saint Graal qu'est l'eFluor et nous avoir ainsi permis de produire une grande partie des résultats de ce mémoire.

Enfin je remercie mes amis proches, Maxime, Carole, Margaux, à tous ceux de l'URBM qui ont participé à ces beaux moments, à ceux qui ne liront pas ces lignes mais qui m'auront fait tenir le cap pendant ces derniers mois, et enfin à Arnaud pour le bonheur qu'il m'apporte au quotidien, pour m'avoir épaulé dans les coups durs et pour sans cesse repousser les limites de mon avenir.

Merci à tous, je ne vous oublierai pas

"If an injury has to be done to a man, it should be so severe that his vengeance need not be feared."

[Nicolas Machiavel, The Prince]

Table of content

List of abbreviations

aBCV	*Autophagy-related Brucella-containing vacuole*
ADCC	*Antibody-dependant Cell-mediated Cytotoxicity*
APCs	*Antigen-presenting cells*
APC	*Allophycocyanin*
CFP	*Cyan fluorescent protein*
CFUs	*Colony Forming Units*
CLR	*C-type lectin receptors*
BALTs	*Bronchi-associated lymphoid tissues*
BCR	*B cell Receptor*
BCV	*Brucella-containing vacuole*
BL3	*Level 3 Biosafety Facility*
BSA	*Bovine Serum Albumine*
CDn	*Cluster of differentiation n*
DAMPs	*Damages-associated molecular patterns*
DCs	*Dendritic Cells*
DMSO	*Dimethyl sulfoxide*
dsRNA	*Double-strand RNA*
DTR	*Diphteria toxin receptor*
eBCV	*Brucella-containing vacuole with endosomal markers*
EE	*Early Endosome*
FACS	*Fluorescence-acivated cell sorting*
FCS	*Fœtal Calf Serum*
FITC	*fluorescein isothiocyanate*
FSC	*Forward scatter*
GALTs	*Gut-associated lymphoid tissues*
GFP	*Green Fluorescent Protein*
HDM	*House dust mite*
HLA	*Human Leukocyte Antigen*
Ig	*Immunoglobulin*
IL	*Interleukin*
IFNγ	*Interferon gamma*
iNKT	*Invariant Natural Killer T cell*
Kan	*Kanamycin*
LAMP1	*Lysosomal-Associated Membrane Protein 1*
LE	*Late Endosome*
LPS	*Lipopolysaccharid*
MAIT	*Mucosae-Associated Invariant T cell*
MALTs	*Mucosae-associated lymphoid tissues*
MHC	*Major Histocompatibility Complex*
Nal	*Nalidixic acid*
NALTs	*Nasal-associated lymphoid tissues*
NK	*Natural Killer*
NLR	*NOD-like receptors*

NO	*Nitric oxyde*
NOD	*nucleotide oligomerization domain receptors*
OCT	*Optimal cutting temperature*
OD	*Optical density*
PAMPs	*Pathogen-Associated Molecular Patterns*
PBS	*Phosphate Buffered Saline*
PRR	*Pattern Recognition Receptor*
Rab7	*Ras-Related 7*
rBCV	*Replicative Brucella-containg vacuole*
rpm	*Rotation per minute*
SE	*Succinimidyl ester*
spp.	*species pluralis*
SSC	*Side Scatter*
ssRNA	*single-strand RNA*
STAT	*Signal Transducers and Activators of Transcription*
T4SS	*Type 4 Secretion System*
TCR	*T Cell Receptor*
TGF	*Tumor Growth Factor*
TIR	*Toll-Interleukin Receptor*
TLR	*Toll-Like Receptor*
TNF	*Tumor necrosis factor*
TRSE	*Texas Red Succinimidyl Ester*
WT	*Wild Type*

Brucella species	Preferential hosts
B. melitensis	Sheep, goats, camels, (humans)
B. abortus	Cattle, buffalo
B. suis	Swine, (reindeer, caribou, rodents)
B. canis	Dogs
B. ovis	Sheeps
B. neotomae	Desert rodents
B. ceti	Seals, dolphins
B. pinnipedialis	Pinnipeds
(B. microti)	Field vole, soil, foxes
(B. inopinata)	Found in breast implant

Table 1: List of *Brucella* species and their respective preferential hosts (Godfroid et al. 2011; Kasper et al. 2015). The species and hosts that were less frequent are in parentheses. The four species that are the most virulent for humans (*B. melitensis*, *B. abortus*, *B. suis* and *B. canis*) are in bold (Kasper et al. 2015).

Introduction

One thing that always struck me is that from the beginning, there is merely one way to create life from scratch, a single difficult way involving a lot of energy and particular events at a specific time. However, I can't imagine how many ways there are to destroy it, or at least to interfere with it. That is why micro-organisms, infections and pathogens were so fascinating to me.

The way humans struggle with those pathogens and the way these bugs fight back keep biologists busy for many many years, and today I am lucky enough to get a little bit closer to the understanding of those mechanisms.

I. Brucella

I.1. *Brucella* genus

The *Brucella* genus are facultative intracellular Gram-negative α-proteobacteria. These unencapsuled bacteria are non-motile rods or coccobacilli which vary in size between 0,5 to 1,5 µm long (Atluri et al. 2011; Kasper et al. 2015). *Brucella* spp. lack of chemotactic system and thus functional flagellum (Seleem et al. 2010). They are able to grow on peptone-based medium at 37°C, in the presence of oxygen and carbon dioxyde. *Brucella* spp. are killed by ionizing radiations – UV light – and heat – pasteurization. However, they are resistant to freezing environment and drought, thus allowing airborne transmission (Kasper et al. 2015). In the environment, *Brucella* survives from six weeks to six months in soil (Kasper et al. 2015).

Unipolar growth

Another particularity is that *Brucella* displays atypical unipolar growth like many *Rhizobiales* (Brown et al. 2012) and an asymmetrical division, a feature that *Brucella* shares with *Caulobacter crescentus*, a model *α- proteobacterium* (Hallez et al. 2004). This characteristic has been previously used to monitor *Brucella* division by using TRSE (Texas Red Succinimidyl Ester) membrane staining (Deghelt et al. 2014). The consequences of an unipolar growth are that the daughter cells appear to display a smaller size and to have different properties than the mother cell, as the repartition of proteins and content both in the membrane and the cytosol is unbalanced, thus participating to the population heterogeneity.

Brucella classification

Brucella species are classified according to their main hosts (Godfroid et al. 2011; Atluri et al. 2011) **[Table 1]**. Among them, four species are particularly infectious for humans, namely in frequency order, *Brucella melitensis* (sheeps, goats and camels), *Brucella abortus* (cattle, buffalo), *Brucella suis* (swine), and *Brucella canis* (dogs) (Pappas et al. 2006; Kasper et al. 2015; Willey et al. 2011; Silva et al. 2011). *B. melitensis*, *B. abortus* and *B. suis* can cause severe arthritis, abortion and infertility in their respective hosts (Godfroid et al. 2011; Moreno 2014; Atluri et al. 2011). This results in huge economic

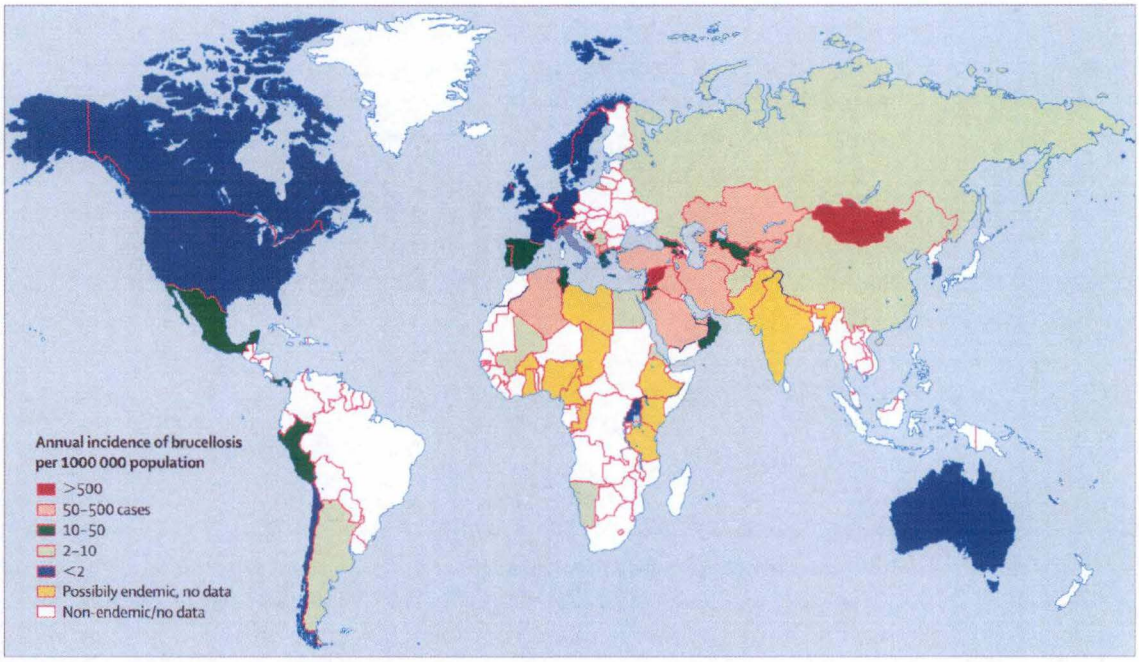

Figure 1: Brucellosis incidence map in year 2006 (Pappas et al. 2006). United States, Australia, Canada, and European countries such as France, Germany and United Kingdom are considered « brucellosis-free » (Pappas et al. 2006)

impacts in countries that rest upon cattle farming due to eradication campaigns and restrictions in commercial exchanges of animal products in countries where brucellosis remains endemic (Godfroid et al. 2011; Atluri et al. 2011).

I.2. Human brucellosis

Brucellosis, also known as undulant fever or Malta fever, is a worldwide zoonotic disease that is transmitted to humans through consumption of infected food – milk essentially – airborne particles or through direct cutaneous contact (Pappas et al. 2006; Atluri et al. 2011; Ariza et al. 2007; von Bargen et al. 2012) and which is mostly caused by *B. melitensis* (Corbel 1997). Transmission between humans is extremely rare and have only been reported through blood or tissue donation, or through breast milk (Kasper et al. 2015; Willey et al. 2011). Farmers, shepherds, veterinarians and laboratory workers are the most likely to be exposed (Kasper et al. 2015).

Brucellosis is especially prevalent and considered endemic in south-west and central Asia, India, South America and Mediterranean countries, but global prevalence is difficult to enlighten due to imprecise diagnosis and inefficient reporting systems in some countries (Kasper et al. 2015; Pappas et al. 2006) **[Figure 1]**.

Symptoms and lesions

The incubation time range from five days to months and leads to an acute febrile state comparable to flu symptoms (Kasper et al. 2015; Willey et al. 2011; Seleem et al. 2010). Months after infection, one could enter into the chronic state of the infection with osteo-articular (nonpyogenic osteomyelitis), genito-urinary, pulmonary, hepatic (hepatomegaly) and splenic (splenomegaly) damages (Kasper et al. 2015; Atluri et al. 2011; Seleem et al. 2010; Pappas et al. 2006). Brucellosis is often diagnosed based on serology analysis to detect protective antibody levels in blood or bone marrow samples. Recovering of the bacteria by blood culture is not accurate enough to be a reliable diagnosis method (Kasper et al. 2015; Seleem et al. 2010).

Treatment and vaccination

The treatment to brucellosis relies on a combination therapy of two antibiotics (rifampicin and doxycycline) for a period of six to twelve weeks (Kasper et al. 2015; Willey et al. 2011; Pappas et al. 2006; Ariza et al. 2007). There is no safe and/or effective prophylaxis treatment for human brucellosis yet, as the live vaccine strains of *Brucella* (S19 & RB51 for *B. abortus*, Rev1 for *B. melitensis*) can induce the disease and display antibiotic resistance (Kasper et al. 2015; Oliveira et al. 2011; von Bargen et al. 2012; Ko et al. 2002). Moreover, antibodies produced by vaccination cannot be differentiated from those produced by a natural infection, which is a huge brake for diagnosis (Seleem et al. 2010; Oliveira et al. 2011).

However, preventive measures can be settled by avoiding unpasteurized dairy products (Kasper et al. 2015). Due to its pathogenicity and the difficulties encountered to prevent the disease, *Brucella* spp. have been classified in the list of possible bioterrorism agents (Kasper et al. 2015; Willey et al. 2011; Moreno 2014).

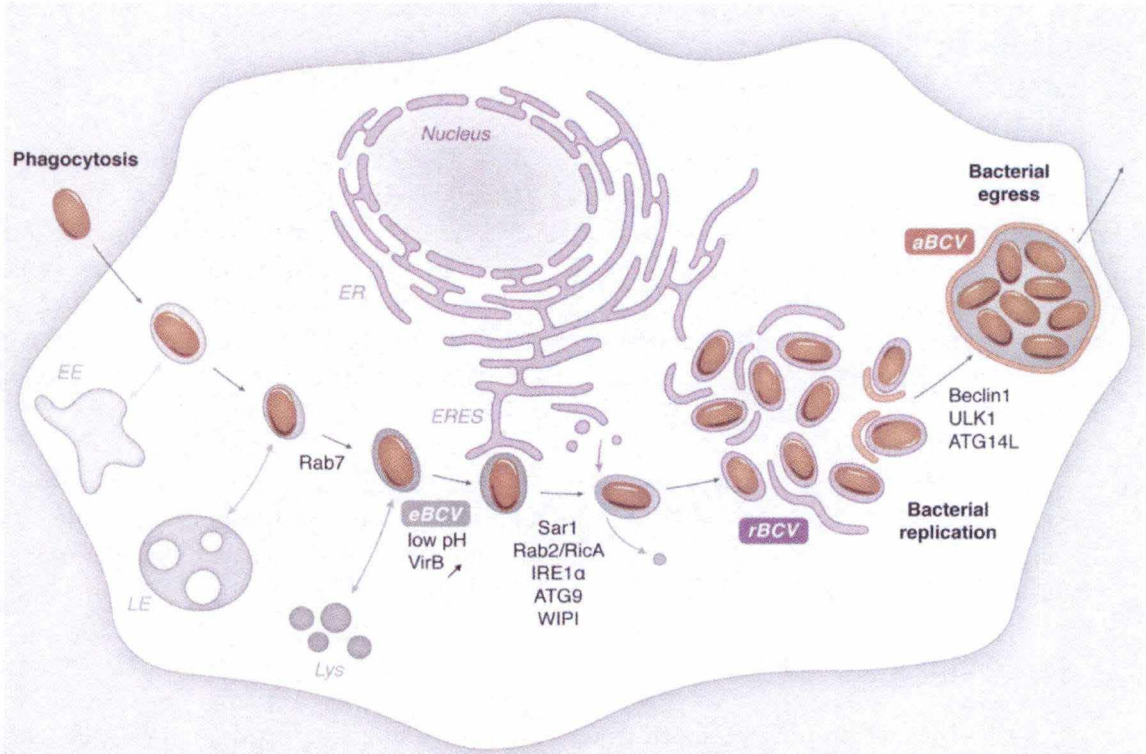

Figure 2: Intracellular trafficking of *Brucella* after internalization (Celli 2015). After fusion with late endosome (LE) and gaining Rab7 markers, the eBCV environment becomes acidic and induces the VirB Type 4 secretion system (T4SS). This allows the eBCV to turn into the replicative niche for *Brucella*, the rBCV. The rBCV may also mature into an autophagy-related BCV (aBCV) and become a double membrane vesicle acquiring autophagy markers such as Beclin1 and ULK1.

I.3. Infection and trafficking

Brucella spp. are able to survive and replicate in lots of different host cells types, as in placental trophoblasts – which causes abortion in infected animals – and in macrophages, leading to the chronic state of infection (Godfroid et al. 2011; Willey et al. 2011). The bacteria makes its way through the mucosal barriers, such as the respiratory tract, skin lesions or the upper digestive tract, depending on the mode of infection (Ke et al. 2015).

Following intranasal infection, *Brucella* infects primarily alveolar macrophages where it is able to strive and replicate (von Bargen et al. 2012; Archambaud et al. 2010; Hanot Mambres et al. 2016). This replication shelter confers to the bacteria a safe spot regarding humoral immunity. The infected macrophages, carrying the *Brucellae*, similarly to DCs, could go upstream to the draining lymph node nearby, where *Brucella* will be able to pursue systemic infection (von Bargen et al. 2012; Archambaud et al. 2010).

In vivo studies showed that after pulmonary infection, *Brucella* persists in the lungs for a few days (four to five days) before quickly reach organs such as the liver or the spleen, the latter being the niche where the bacteria persists despite the immune responses and leads to chronic infection, while the lungs and the liver are rapidly cleared out of the bacteria (von Bargen et al. 2012; Hanot Mambres et al. 2016; Hanot Mambres et al. 2015). Little is known about the way *Brucella* travels from an organ to another, even though red blood cells seems to be carriers following intraperitoneal infection (Vitry et al. 2014).

In vitro, studies on immortalized cell lines showed that *Brucella* was able to infect and replicate in human HeLa cells and murine RAW264.7 macrophages, following a two-step infection process: a non-proliferative state where the bacteria remain steady at low levels, and a proliferative state where the bacteria replicate intensively (Deghelt et al. 2014; Celli 2015; Comerci et al. 2001; Delrue et al. 2001).

After adhesion with the host cell, involving adhesin, fibronectin and sialic acids (Castañeda-Roldán et al. 2006), and its phagocytosis by competent cells, *Brucella* is enclosed in a *Brucella*-containing vacuole (BCV), with early endosome markers like Rab5 (Celli 2015; Ke et al. 2015).

This BCV will lose early endosome markers and replace them with late endosome markers, like LAMP1 (Lysosomal-Associated Membrane Protein 1) and Rab7 (a small GTPase) to mature into a BCV displaying endosomal markers (eBCV). Brucella is able to control the conversion of eBCV into a replicative vacuole (rBCV) having endoplasmic reticulum markers, twelve hours after infection (Celli 2015; Starr et al. 2008; Starr et al. 2012). This rBCV subsequently turns into an autophagy-related compartment (aBCV), with autophagy markers such as ULK1 or Beclin1 (Celli 2015; Starr et al. 2008; Starr et al. 2012) **[Figure 2]**. This aBCV might be involved in the cell-to-cell spreading of Brucella after completing its intracellular lifecycle (Starr et al. 2012).

The eBCV maturation seems to be triggered upon acidification to pH 4 to 4.5, and the following induction of the virulence factor VirB T4SS (type IV secretion system) essential for survival and replication inside host cells (Boschiroli et al. 2002; Sieira et al. 2000; Celli et al. 2003; Salcedo et al. 2008). In RAW264.7 macrophages, the non-proliferative state is reflected in an arrest in the G1 phase during the first six hours post-infection, in the eBCV (Deghelt et al. 2014). Bacterial growth resumes at the end of the eBCV trafficking, while division and proliferation occurs in the rBCV (Deghelt et al. 2014).

II. Immune system

II.1. General definitions

The immune system is a full range of evolved mechanisms that are settled to protect an individual from microbes – bacteria, virus and other bugs – and their virulence factors, in order to keep the integrity of the system. The principal actors of immunity are the physical barriers, the lymphoid organs (spleen, thymus, lymph nodes and associated lymphoid tissues), and the immune cells (Kasper et al. 2015; Willey et al. 2011).

Non-specific defenses are settled by the organism and refer to the barriers, the secretions and the normal flora that are present in the body. The skin represents an effective mechanical barrier (in addition to the variety of antimicrobial factors), as well as the mucosal layer of the mouth and respiratory tract (this is tragically shown by the increasing exposure to pathogens in cystic fibrosis patients where the respiratory mucosae is badly impaired) (Zabriskie 2009; William 2013).

The primary lymphoid organs are sites where pre-T and pre-B cells mature into naïve T and B cells in the absence of non-self antigens. These sites are the fetal liver, the bone marrow and the thymus. The naïve B and T cells thus leave the primary lymphoid organs, following development signals to rearrange their genetic material, and generate a repertoire able to recognize a great variety of non-self antigens. Finally, they migrate into the tissues and settle in secondary lymphoid organs which are the lymph nodes, the spleen, the appendix, tonsils, MALTs (but also GALTs, BALTs, NALTs), or Peyer's patches (William 2013).

A typical healthy immune system will have three main characteristics:

- A **diversified set** of antigen receptors to be ready to face any pathogen (or nearly), recognizing the microbial key molecules. These receptors named « PRR » (Pattern Recognition Receptors) includes mostly the Toll-like receptors, which recognize specific sets of molecular motifs associated with microbial agents (William 2013)

- The ability to conserve **immune memory**, after primary exposition with an antigen. This leads to an antibody response that is set faster, with a wider magnitude and affinity for the antigen (William 2013).

- Immunologic **tolerance** regarding self-antigens, with an ability to discriminates between antigens expressed on foreign substances and antigens expressed by the host tissues. This involves, for exemple, the elimination of cells reactive towards self-antigens, or the anergy process (inactivation of reactive cell) (William 2013).

The immune system may be split in two categories, namely the innate immune system, and the adaptive immune system (Kasper et al. 2015; Willey et al. 2011). When dysregulated, the immune system may give rise to uncontrolled infections or autoimmune disorders (William 2013).

Localization	TLR type	Ligand
Plasma membrane	TLR1	Triacyl lipoprotein
	TLR2	Lipoprotein
	TLR4	LPS
	TLR5	Flagellin
	TLR6	Diacyl lipoprotein
	TLR11	Profilin-like molecules
Endolysosome	TLR3	dsRNA
	TLR7/TLR8	ssRNA
	TLR9	CpG-DNA
	TLR10	Unknown

Table 2: List of Toll-like receptors, their specific localization and ligand (Kasper et al. 2015). Origins of these ligands are either bacterial, viral, parasitic, protozoan or human.

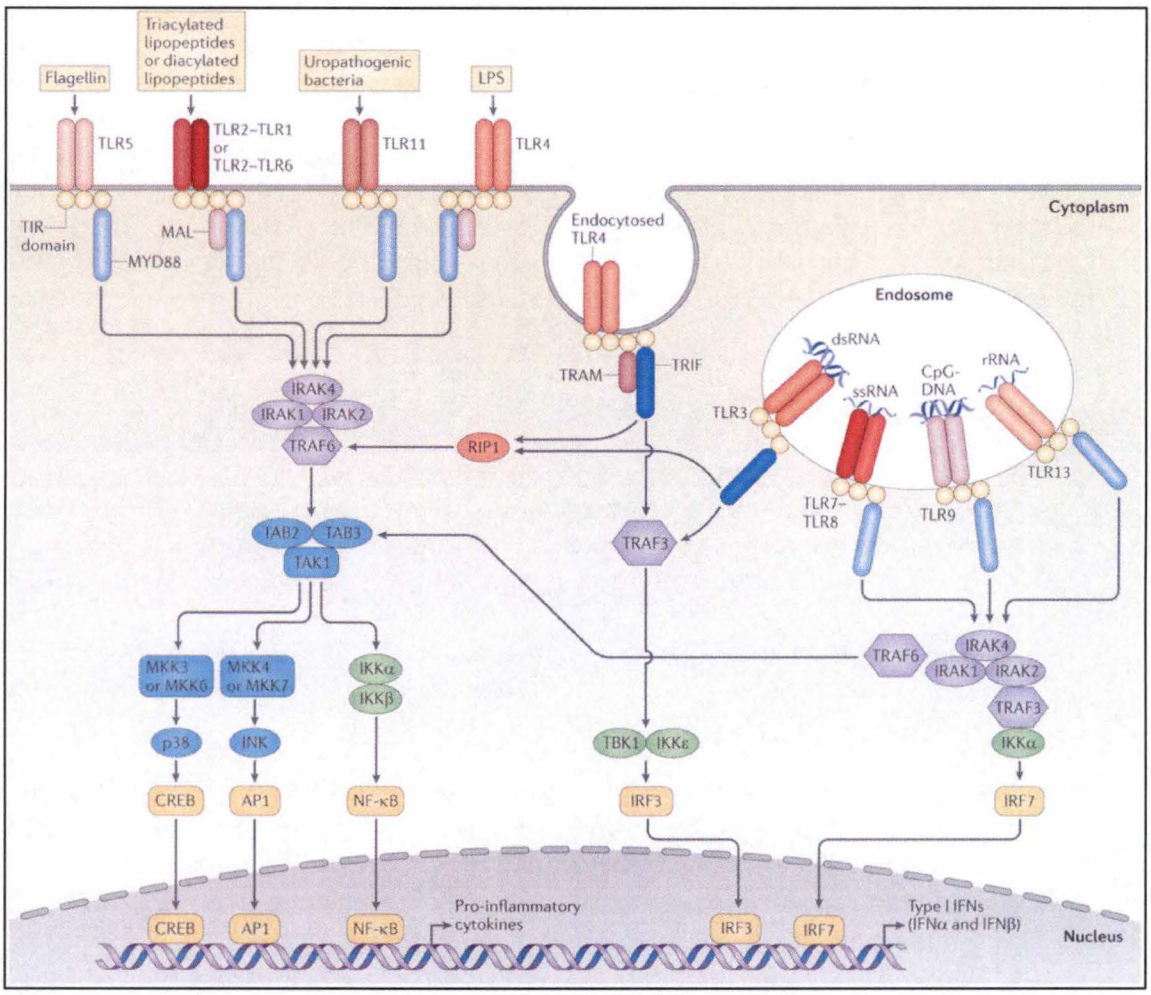

Figure 3: Toll-like receptors signaling pathways (O'Neill et al. 2013). Specific TLRs or combination of TLRs recognize different pathogen motifs and lead to specific signaling pathways, through TIR domains or adaptor protein such as MyD88. The principal outcomes are the induction of pro-inflammatory cytokines and type I interferons.

Innate immune system

The innate immune system is a well-conserved immune recognition system which relies on PRR-carrying cells (Pattern Recognition Receptors) to detect pathogens through their PAMPs (Pathogen-Associated Molecular Patterns) and therefore trigger mechanisms leading to pathogen elimination (Kasper et al. 2015; Willey et al. 2011).

Adaptive immune system

The adaptive immune system is a set of immune responses mediated by B and T lymphocytes, and based on specific antigen recognition by receptors produced by genetic rearrangement during the development and the lifetime of an individual. Specialized antigen-presenting cells are also involved in the orchestration of this immune response (Kasper et al. 2015; Willey et al. 2011). The specific immune response is divided into humoral and cellular immunity (Zabriskie 2009).

II.2. Innate response actors

The innate immune response involves lots of cell types with specific functions, such as the natural killer (NK) cell lymphocytes, the monocytes and macrophages, the dendritic cells (DCs), neutrophils, basophils, eosinophils, tissue mast cells and epithelial cells (Kasper et al. 2015).

The detection of PAMPs is done through PRR molecules, including the Toll-Like Receptors (TLR), the C-type lectin receptors (CLR), or NOD-like receptors (NLR). Macrophage scavenger receptors are able to opsonize the bacteria et activate the complement cascade. The TLR proteins can be found on macrophages, DCs, B cells but also on lung epithelial cells. In Human, eleven TLR has been identified, all of them displaying specific recognition patterns **[Table 2]** and pathways **[Figure 3]** (Kasper et al. 2015; Swain et al. 2012). For instance, the TLR2 recognizes bacterial lipopeptides whereas TLR5 senses flagellin (O'Neill et al. 2013).

Macrophages are phagocytic cells that can be found in all the tissues but particularly in the lymph node, the spleen, the bone marrow, the lungs (as alveolar macrophages) or the liver. The main function of macrophages are to phagocytose invading organisms, dead cells, particles and antigens (Zabriskie 2009). They are considered the first line of defense due to their ability to kill pathogens through the production of nitric oxide (NO), reactive oxygen species (such as superoxide anions, hydroxyls groups, oxygen triplets, hydrogen peroxide) hydrolases and other degrading enzymes, and inflammatory mediators such as IL-1, TNF-α, IL-6, or IL-12 (Kasper et al. 2015; Zabriskie 2009). Macrophages are also a very plastic population which is able to change its phenotype under certain conditions (Holt et al. 2008; Hussell & Bell 2014).

The **dendritic cells** (DCs) are myeloid antigen-presenting cells (APCs) that play a role in the innate immunity as an initiator when they are immature, by secreting high levels of cytokines such as IL-12, IL-23 and TNF-α after recognition and ingestion of infectious agents (Zabriskie 2009). The TLR engagement upregulates expression of MHC Class II, which improve the antigen presentation ability of DCs (Kasper et al. 2015).

Cytokines	Receptor	Cell Source	Cell Target	Biologic Activities
IL-1	Type I and Type II IL-1r	Macrophages, B cells, epithelial and endothelial cells	All cells	Upregulates adhesion molecule expression, neutrophil and macrophages emigration
IL-6	IL-6r	Macrophages, B cells, epithelial and endothelial cells	T cells, B cells, epithelial cells, macrophages	T and B cell differentiation and growth, myeloma cell growth
IL-12	IL-12r	Activated macrophages, DCs, neutrophils	T cells, NK cells	Induction of T_H1 helper cell formation, increase $CD8^+$ cytolytic activity, upregulation of IFNγ and downregulation of IL-17
IL-17	IL-17r	$CD4^+$ cells	Fibroblasts, endothelium, macrophages	Enhance cytokine secretion
TNF-α	TNFRI, TNFRII	Macrophages, basophils, eosinophils, NK cells, B cells, T cells	All cells	Enhance leukocyte cytotoxicity and NK cells functions, pro-inflammatory cytokines induction
IFNγ	Type II interferon receptors	T cells, NK cells	All cells	Regulation of macrophages and NK cells activation, stimulate Ig secretion by B cells, induction of MHC II, T_H1 cell differentiation

Table 3: Adaptation of the cytokines table and their receptors (Kasper et al. 2015). For clarity of exposition, only relevant data are included in this table.

Once activated, the DCs carry the pathogenic antigens to the peripheral lymphoid organs in order to present them to T cells (Zabriskie 2009). Facing intracellular pathogens, the IL-12 and IL-23 cytokines bind to their receptors on Natural killer cells, which will secrete IFNγ. In combination with TNF-α, IFNγ will activate macrophages, through a STAT-1 dependant pathway, which are then able to kill intracelluar pathogens (Zabriskie 2009).

Natural killer cells (NK) are large lymphocytes which specifically target cells lacking of MHC Class I (Major Histocompatibility Complex) molecule at their surface membrane, with no need to either antigen or antibody stimulation (Zabriskie 2009) but can also be activated directly by pathogens (through TLR recognition) or inhibitor receptors. This lack of HLA/MHC I might be found, for example, in cells γected with a virus. Indeed, NK deficiencies in animals induce a greater incidence of viral infections and malignancy cells (Zabriskie 2009). The killer function is inhibited when the MHC Class I is found (William 2013). They are also involved in ADCC (Antibody-dependant Cell-mediated Cytotoxicity), when a targeted cell is coated with antibodies (Kasper et al. 2015; William 2013).

NK T cells are NK cells expressing CD3 (Cluster of Differentiation 3) and invariant TCR-α chains. The TCR recognizes lipids of intracellular bacteria, like *Listeria monocytogenes* or *Mycobacterium tuberculosis*, when presented by APCs. After activation, they secrete IL-4 or IFNγ which leads to DCs activation (Kasper et al. 2015).

Neutrophils, **eosinophils** and **basophils** are granulocytes that are involved in inflammation and the amplification of innate immunity responses. Those granulocytes are derived from different subclasses of progenitor cells and acquire specific cytoplasmic and nuclear morphology.

- **Neutrophils** are attracted to the site of infection by, *inter alia*, cytokines produced by T_H1 cells (introduced later) and are involved in direct tissue damages by secreting superoxide radicals and enzymes (Zabriskie 2009).

- **Eosinophils** play a role in cytotoxicity towards parasitic organisms and the regulation of inflammatory responses. They complete their differentiation under IL-5 signals, which are cytokines released by T_H2-oriented cells (introduced later) (William 2013). Following helminthic infection, eosinophils release major basic protein, eosinophil cationic protein and eosinophil peroxidase, which provoke tissues damages both to the host and the parasite (William 2013).

- **Basophils** face bacterial and viral infection with IL-4 cytokines (This stimulates the T_H2 T cell differentiation, which will be introduced later) and participate to the activation of the complement (Kasper et al. 2015). They are able to bind antibodies to their surface, and the recognition of a circulating antigen by these antibodies induces the release of mediators such as histamine, serotonie and enzymes involved in anaphlactic-like responses or allergic responses (William 2013).

The principal outcomes of the innate immune response are the activation of the complement cascade, the production of cytokines and antimicrobial peptides, and the maturation of DCs into antigen-presenting cells. The cytokines produced display a large panel of biologic activities **[Table 3]** (Willey et al. 2011; Kasper et al. 2015).

II.3. Adaptive response actors

The two main actors of the adaptive immunity are T cells, which are responsible for cellular immunity, and B cells for humoral immunity. The first exposure with an antigen leads to a quickly and emphasized response of the system when exposed to the same antigen a second time, namely the immunologic memory (Kasper et al. 2015).

The **T lymphocytes** can differentiate in thymus into $CD8^+$ cytotoxic T cells (for lysis of infected cells) and $CD4^+$ Helper T cells (to help $CD8^+$ and B cell development in B cell follicles) (Zabriskie 2009; William 2013). The thymic T cell precursors can rearrange the TCR genes and split into two different T cells subsets, whereas the express the TCR-αß chains (the majority, differentiating into $CD4^+$ or $CD8^+$ cells) or TCR-γδ chains (William 2013).

The $CD4^+$ helper αß-positive T cells regulates $CD8^+$ αß-positive T and B cells by producing cytokines and through direct contact (Kasper et al. 2015; Swain et al. 2012). The $CD8^+$ cytotoxic T cells are able to kill cells through the secretion of perforin (to promote lysis of the cell by inserting itself in the membrane) and granzymes (William 2013; Kaufmann 2007).

The TCR-γδ lymphocytes are in minority in lymphoid organs but abundant in mucosal immune system. Their functions are less known, even though they might be involved in the recognition of intracellular bacteria antigens and the production of IL-17, TNF-α or IFNγ (Vantourout & Hayday 2013; Kasper et al. 2015). We can also argue that the γδ cells play a more relevant role in the innate immune response, as the IL-17 cytokines are produced quickly after infection (Peng et al. 2008).

Mature DCs are involved in the activation and differentiation of naïve T cells into effector T cells after the presentation of the antigen through their MHC and delivery of costimulation signals. If the antigen is presented by the MHC Class I, cytotoxic $CD8^+$ T cells will be activated to induce cell lysis. On the other hand, if the antigen is presented by the MHC Class II, Helper $CD4^+$ T cells will be activated and orchestrate the immune response by activating B cells (Kasper et al. 2015).

B cells express surface immunoglobulins, which are acting as B cell receptors (BCR) for antigens. However, B cells do not need those antigens to be processed by APCs and can bind them in their native form. They are also able to act like APCs and present antigens to $CD4^+$ T cells. The primary function of B cells is the production of antibodies. In their immature form, B cells only express IgM and IgD of low affinity, and it is only after activation and maturation that they are able to synthesize IgG, IgA (secretory Ig) and IgE of high affinity (Kasper et al. 2015).

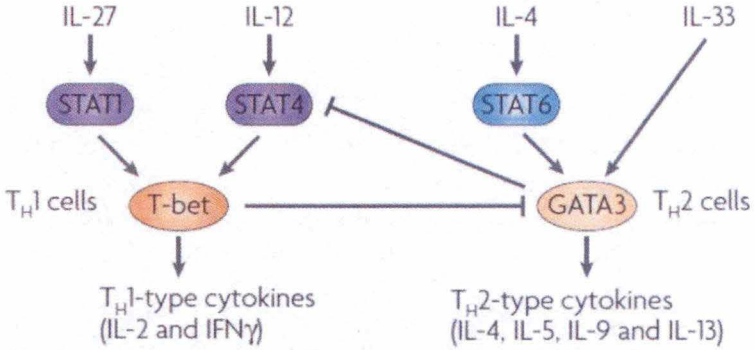

Figure 4: Pathway of cross-inhibition between the T_H1 and T_H2 responses (Potemberg et al. 2015). The T_H1 response transcription factor T-bet downregulates the T_H2 transcription factor GATA3, thus committing the cell to a T_H1 function. GATA3 has the same downregulating role on STAT4, an intermediate in the T_H2 pathway (Barnes 2008).

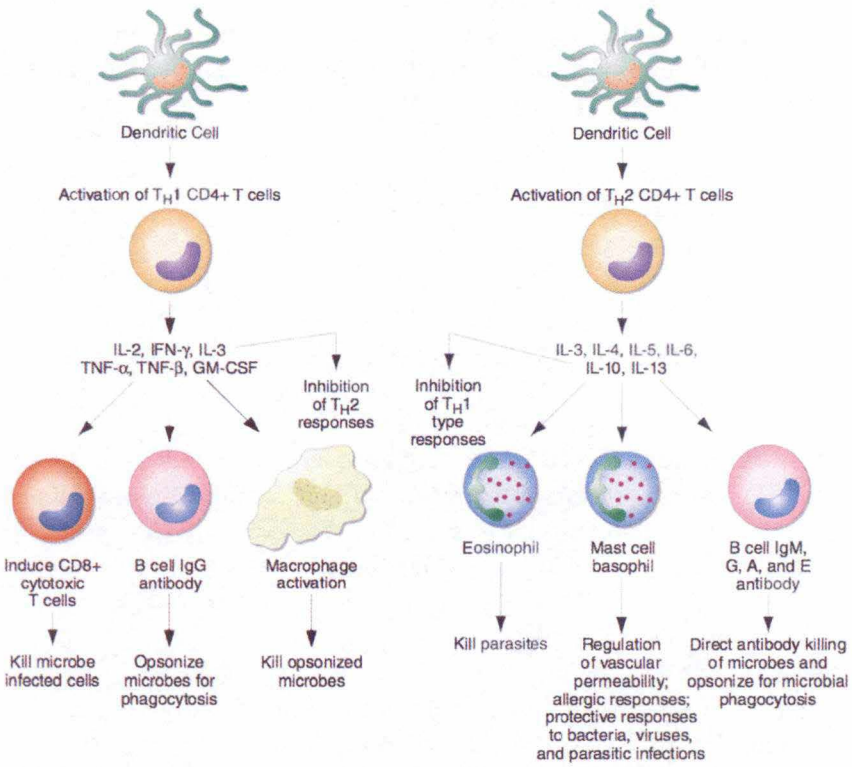

Figure 5: T_H1 and T_H2 differentiation and biological effects (Kasper et al. 2015). Both T_H1 and T_H2 T cells secrete specific cytokines that will impact on different cell types to induce anti-microbial response for T_H1, and allergic or anti-parasitic response for T_H2.

T_H1 Response

The T_H1 response is settled in response to viruses and intracellular bacteria (William 2013). This results from the exposition of naïve T cells to IFNγ and IL-12, which induce the expression of T-bet, a transcription factor that favors the switch of naïve T cells into T_H1 cells, and downregulates the transcription factor involved in the T_H2 pathway, in a process called cross-inhibition (Barnes 2008; Lazarevic & Glimcher 2011) **[Figure 4]**. The T_H1 response will result in a production of IFNγ which will reinforce the T_H1 switch, upregulate MHC Class I and Class II expression and induce immunoglobulin isotype switching in B cells (Kasper et al. 2015; Swain et al. 2012; Zabriskie 2009) **[Figure 5]**. In humans, the T_H1 cytokine profile is mainly directed toward protection against intracellular pathogens (Zabriskie 2009).

The T_H1 response also plays a role in the activation of macrophages, through TLR ligands and IFNγ signals which will polarize macrophages into proinflammatory "classically activated macrophages" (M1 macrophages) (Biswas & Mantovani 2012). These M1 macrophages are characterized by the secretion of proinflammatory cytokines such as IL-1, IL-12, IL-23 and TNF-α (Holt et al. 2008; Hussell & Bell 2014; Muraille et al. 2014), the expression of iNOS/NOS2, ROS, RNI (reactive nitrogen intermediate) and a strong microbicidal activity (Biswas & Mantovani 2012). The classically activated macrophages display an anaerobic glycolytic metabolism (to trigger microbicidal activity in hypoxic tissues), low fatty acid oxidation, and iron retention (Biswas & Mantovani 2012; Odegaard & Chawla 2012).

T_H2 Response

The T_H2 immune response is mainly involved in the protection against parasitic helminths and in response to allergens (Chen et al. 2012; Palm et al. 2012; William 2013). This switch is triggered by IL-1 or IL-6 exposure, lesion in the epithelium releasing cytokines such as IL-33, and the recognition of DAMPS (Damages-Associated Molecular Patterns) (Liew 2012; Zabriskie 2009). The T_H2 cells secretes cytokines like IL-4, IL-5 and IL-13, in order to promote the IgE isotype switch of B cells (involved in allergies and anti-parasitic responses), and the recruitment of eosinophils, mast cells and basophils (Kasper et al. 2015; Swain et al. 2012; Zabriskie 2009) **[Figure 5]**. Therefore, the T_H2 cytokine profile interacts with diseases characterized by overproduction of antibodies such as IgE (Zabriskie 2009).

IL-4 and IL-13 cytokines are perceived through receptors present on the surface of macrophages and induce a STAT-6-mediated signal to polarize macrophages into "alternatively activated macrophages" (M2a macrophages) characterized by the expression of Arginase1 and chitinase (William 2013; Biswas & Mantovani 2012). These M2a macrophages are involved in the resolution of inflammation, healing of tissue damages, and the T_H2 response through immunoregulatory functions (Holt et al. 2008; Hussell & Bell 2014; Muraille et al. 2014; Biswas & Mantovani 2012). The alternatively activated macrophages display fatty acid oxidation-based metabolism (for tissue repair), and an iron-export activity (for immunoregulation) (Biswas & Mantovani 2012; Odegaard & Chawla 2012). The glucose availability in the M2a macrophages has been showed to

enhance the intracellular bacteria survival such as *Brucella* (Xavier, Winter, Spees, Den Hartigh, et al. 2013). The T_H2 response is often opposed to the outcomes of the T_H1 response in some infections with microorganisms that are intracellular pathogens of macrophages. As a result, a T_H2-oriented response may be associated with failure in the control of infection (William 2013).

T_H17 Response

The T_H17 response is mediated by IL-17-producing T cells and is a rapid immunity response settled in order to face extracellular bacteria (William 2013). The T_H17 cells are involved in the granulocytes recruitment to enhance the primary inflammatory response (William 2013). T_H17 cells also produce IL-22 and IL-26. The T_H17 response has been previously described to be involved in auto-immune diseases (Ouyang et al. 2012).

II.4. Allergic Asthma

Asthma is an inflammatory syndrome characterized by generalized and reversible airflow obstruction, wheezes, dyspnea and cough (Zabriskie 2009). It is one of the most common chronic diseases as it affects around 300 million people worldwide. Individuals are mostly sensitized to house dust mite (*Dermatophagoides pteronyssinus*), molds (such as *Alternaria alternata*) animal fur, fungi, cockroach epithelium or pollen (Kasper et al. 2015; Zabriskie 2009). Inhaled allergens cause the mast cells to be activated upon binding with IgE, which leads to direct release of bronchoconstrictor mediators, and delayed airway oedema et acute inflammatory response with increasing levels of neutrophils and eosinophils (Kasper et al. 2015). Moreover, some of these antigens, such as *Alternaria alternata*, display protease activities, which induce damages to epithelia.

Histologically, allergic asthma is characterized by a thickness of the airways, generalized oedema, smooth muscle and mucus gland hypertrophy, and denudation of the epithelium (Zabriskie 2009). The airway mucosa of asthmatic patients is infiltrated with activated eosinophils and mast cells, and T lymphocytes. The inflammation spreads from the trachea to terminal bronchioles, but remains predominant in bronchi (Kasper et al. 2015).

In a healthy pulmonary tissue, the T_H1 response is preponderant under the effect of IL-12 and TNF-α. However, in individuals predisposed to develop a T_H2 and after exposure to some antigens, the immature DCs can process the antigens and present the peptides to $CD4^+$ T cells in local lymph nodes (through interaction with the CD28 receptor), which will promote T_H2 response.

The T_H2 cells promote eosinophils recruitment and survival as well as the maintenance of mast cell populations in the airways, through the release of IL-3, IL-5, IL-4, IL-13 and TNFα (Kasper et al. 2015; Zabriskie 2009). The IL-4 and IL-13 cytokines are also the key stimuli for B cells to switch to IgE production (Zabriskie 2009).

As previously described, the local switch to T_H2 phenotype in lungs prevent the T_H1 phenotype, which is protective against a wide range of pathogens (Habibzay et al. 2013; Barnes 2008; Kasper et al. 2015).

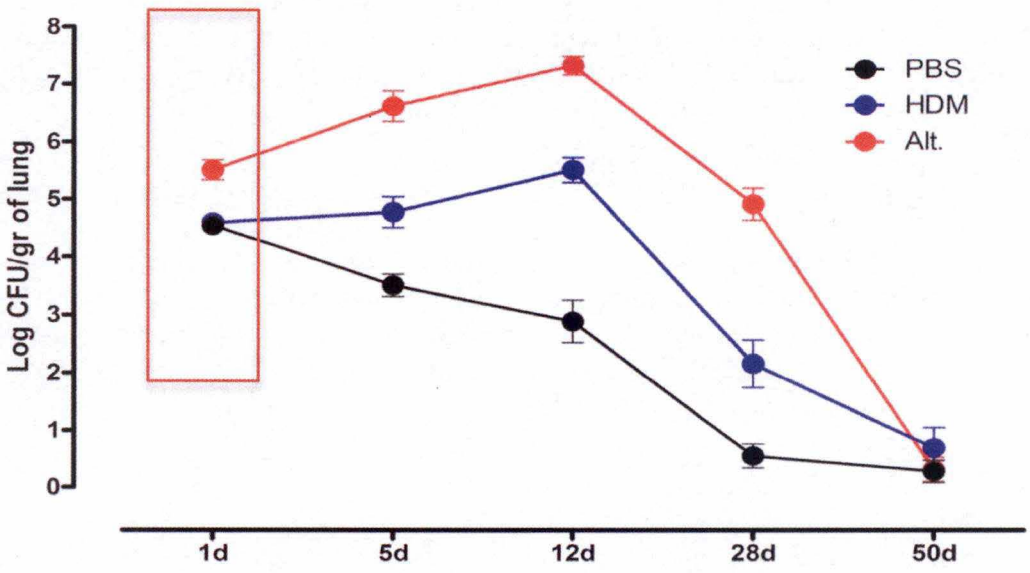

Figure 6 : Comparison of CFUs kinetics after infection with low doses of *Brucella melitensis* (2.10^4 CFUs) in wild-type mice (in black) and sensitized mice for allergic asthma, with house dust mites extract (in blue) or with *Alternaria alternata* extract (in red) (Machelart 2016). After only 24 hours, mice sensitized with *Alternaria alternata* extract display one Log higher of CFUs than the WT mice.

The T_H2 switching also leads to the polarization of macrophages into M2a macrophages, which display a weaker ability to get rid of intracellular bacteria (Habibzay et al. 2013).

Studies showed that exposure to viral infections such as measles, thus leading to IFNγ and T_H1 cytokines, have a negative impact on the apparition of T_H2 cytokine profiles, thus reducing allergy symptoms (Zabriskie 2009). This might explain the increase of allergic events in developed countries where the infections rates are dropping (Zabriskie 2009).

Use of allergic asthma as a positive factor for Brucella growth

The impact of allergic asthma on the ability of the host to control an intranasal infection by *Brucella* in the mouse model has been previously investigated by Potemberg (Potemberg et al. 2015). Asthma sensitization appeared to inhibit the control of the *Brucella* infection by the immune system, and lead to a significant increase of the bacterial load in the lungs of asthmatic mice (Potemberg et al. 2015). Indeed, the induction of allergic asthma triggers a switch of the T_H response to a T_H2-oriented response.

As previously discussed, the T_H2 switch prevents the orientation of the T_H1 response (Barnes 2008), which is the preferential response to control *Brucella* infection (Kasper et al. 2015). Thus, the allergic asthma inhibits, in some sorts, the protective response against *Brucella*, allowing the bacteria to strive and replicate, safe from immunity harm.

In his Master thesis, Potemberg used HDM (House dust mites) extracts to induce allergic asthma (Potemberg et al. 2015). The allergic phenotype was confirmed by the observation of different characteristics found in asthmatic patients such as the massive recruitment of eosinophils in histology sections of the lungs, the activation of the respiratory epithelium, and the production of mucus and IgE.

However, the extract of *Alternaria alternata* (an opportunistic fungus) appears to induce a stronger allergic phenotype than the HDM does (Machelart 2016). This induction has been assessed for 50 days with mice inoculated intranasally with PBS as control, with HDM extract and with *Alternaria alternata* extract. These mice – control and asthmatic – were then infected with low dose of mCherry-expressing *B. melitensis*. Mice were sacrificed at specific timing for CFUs counting.

Only 24 hours after infection, the difference in CFUs between the control group and the asthmatic mice sensitized with *Alternaria alternata* extract is no less than one Log, while mice sensitized with HDM extract show no differences in CFUs with the control mice **[Figure 6].** The gap gets wider at 5 days post infection with a striking difference of mostly three Logs between the control group and the asthmatic group sensitized with *Alternaria alternata*. These results suggest that the induction of asthma promotes a safer environment for *Brucella* to grow and strive in the lungs, for at least fifty days after infection.

III. Mice models and infection

III.1. Model choice

Choosing the proper animal model is an important decision when it comes to *in vivo* studies. In a model of infection with a class III pathogen like *Brucella*, it is crucial to handle and store animals in a level III biosafety facility. This might represent a real challenge if you want to investigate *Brucella* infection in its natural hosts, like sheeps or cattle. That is why the use of a model animal is unavoidable.

Studies focusing on *Brucella* infection have already used several animal models to investigate its impacts on the organism. Those animal models were mice, rats, guinea pigs (he most susceptible for *Brucella* infection) or monkeys (Silva et al. 2011).

Previously in our research group, *in vivo* studies of *Brucella* used mice as a model (Vitry et al. 2014; Hanot Mambres et al. 2016). For the sake of continuity, keeping the same model is the logical choice. However, the mouse model has many advantages.

First of all, mice are susceptible to *Brucella*, which means that an immune response is settled following infection (Silva et al. 2011). This is not surprising as mice are natural hosts for strains of *Brucella* such as *B. neotomae* and *B. microti*. Mice can also be genetically manipulated to create immune-deficient individuals by knock-out techniques (Silva et al. 2011), which is an important feature in immunity and host-pathogen interactions studies. Last but not least, mice are easy to breed, store and manipulate under a hood for different routes of infection, such as intraperitoneal, digestive or intranasal routes (Silva et al. 2011).

However, every model has its limits. Strains of mice used are practically clonal and don't take into account the heterogeneity of the population. Also, by standardizing the conditions of the infection, we get rid of any influence of the environment, which plays a huge role in infection and immunity.

Finally, the doses used for the infection are at way higher levels than the one that could be encountered naturally. Despite all this, standardization is the only way to monitor differences between groups that would remain unseen in an heterogeneous population.

We mostly used C57BL/6 mice for our studies. This strain of mice has an innate preference for T_H1-oriented T_H response, which makes them a little bit more resistant to bacterial infection and helps us to detect specific defense mechanisms of their immune system (Silva et al. 2011). Our objectives were to compare wild-type (immune-competent) mice with immuno-deficient ones. These knock-out mice were deficient for key elements involved in the detection of the bacteria, the signaling pathway, or the T_H response.

III.2. Respiratory tract

The respiratory tract is one of the area the most exposed to pathogens. The air entering the lungs is constantly filled with particles and pathogens present in the environment. However, commensal flora – community of micro-organisms that does not cause harm to its host – also resides in the lungs, but does not trigger any inflammatory response that might be deleterious for the lung tissue. The immune response has to be balanced not to damaging the barrier and thus opening the way to pathogens, but also to fight a pathogen when it is detected (Williams 2012).

Upper Airways

There is two main parts in the respiratory tract. The first part is the upper (or conducting) airways, which begin with the oral and nasal cavities that rejoin into the larynx and the trachea. The trachea then divides into two bronchi, both dividing into smaller ducts (bronchioles). The bronchioles are split into terminal bronchioles (Williams 2012).

The role of this system is to humidify and warm the air that reaches the lower part of the lungs. The ciliated epithelium of the airways mucosa also allows the clearance of any pathogen and/or particles that might be present in the inhaled air. The mucus produced by the mucosa traps those debris, and the clearance movements of the ciliated epithelium (mucociliary apparatus) sweep it up to the larynx where it can be swallowed (Williams 2012).

Lower Airways

The second part is the lower airways, responsible for the gaseous exchange system, and is composed of those terminal bronchioles leading to alveolar ducts and alveoli. The alveoli sacs are made of a thin layer of epithelial cells and are highly vascularized (Williams 2012).

Lung Immunity

The mucus covering the airways is the principal barrier preventing the entry of pathogens. It is composed of mucin, a glycosylated protein which hinders attachment of the pathogens to the epithelium, antimicrobial peptides and IgA to neutralize bacteria, whether they are pathogenic or commensal. Indeed, the dimeric IgA are able to neutralize antigens but are poor inducers of the immune response, which allows to avoid any disproportioned inflammatory response and keep the lungs integrity (Williams 2012). Different mechanisms are settled by the airway immune system to face pathogens (Grubor et al. 2006):

- **Surfactant proteins** are produced by the airways epithelium and include collectins, lysozyme (which cleaves glycosidic bonds of the bacterial peptidoglycan) and lactoferrin (which inhibits growth of iron-requiring bacteria) (Grubor et al. 2006). Collectins include the hydrophilic SP-A, which induce the formation of ROS (Haagsman 2002) and disruption of microbial cell membrane, and SP-D, which induce the aggregation of pathogens to enhance phagocytosis (Wright 2004; Holmskov et al. 2003).

- The **complement cascade** might be activated directly or indirectly by pathogens and results in their opsonization for phagocytosis, or the assembly of a pore-forming membrane attack complex (Hoffmann et al. 1999), through the classical pathway (necessiting an antibody recognition), the alternative pathway (induced directly by the micro-organism) or the lectin pathway (requiring mannose-binding protein) (Hoffmann et al. 1999).

- The **cationic peptides** are produced by the airway epithelium. It includes defensins such as ß-defensins. They are able to kill or neutralize pathogens by binding to the negative membrane of bacteria, due to their positive charges, and form holes by pertubing the lipids assembly (Brogden et al. 2003; Grubor et al. 2006).

- **Anionic peptides** require zinc for maximal activity (Brogden et al. 2003) and act as charge-neutralizing molecules, even though their role in bacterial killing is not well known. Hypothesis suggest that the positively-charged zinc might interact with the negatively charged bacteria membrane, cross the membrane and inhibit the ribonuclease activity (Brogden et al. 2003)

The lungs have its own proper immune system, with regulatory $CD4^+$ T cells, interstitial and alveolar macrophages and $\gamma\delta$ T cells. The alveolar macrophages are the predominant population of immune cells in the alveoli, and are able to migrate to the lymph nodes following intracellular *Brucella* infection (Archambaud et al. 2010). To prevent inflammation under normal conditions, alveolar macrophages secrete anti-inflammatory cytokines such as IL-10 and TGF-ß. These cytokines target DCs and keep them inactivated. Regulatory $CD4^+$ T cells are mostly immunosuppressive by secreting IL-10 to reduce allergic inflammation (William 2013).

The $\gamma\delta$ T cells have a regulatory role, but they are also able to promote inflammation following bacterial infection through the production of IFNγ or IL-17 (Vantourout & Hayday 2013). The IFNγ therefore activates macrophages, which produce IL-12 to promote the T_H1 switching of the $CD4^+$ T cells.

III.3. *Brucella* infection models

Previous studies have used intraperitoneal infection models (Vitry et al. 2014). However, this route of infection remains non-natural and bypasses mucosal immune system. More recently, intranasal infections have been settled (Hanot Mambres et al. 2016; Hanot Mambres et al. 2015) which represents a more natural way of infection.

We studied the first 24 hours following intranasal infection with *Brucella melitensis* at low doses (2.10^4 colony forming units) to investigate the impact of immunity on *Brucella*. Unfortunately, we had to use higher doses (2.10^7 colony forming units) to be able to detect *Brucella* by flow cytommetry and histology analysis.

IV. What do *we* know?

Several studies have been performed to improve our knowledge about *Brucella* infection and control, leading us today to do this Master thesis. It has been previously showed that in a mouse experimental model and following intranasal infection, *Brucella* primarily infects alveolar macrophages on the lungs, before slowly disseminating to the spleen and liver (von Bargen et al. 2012; Archambaud et al. 2010). Entering the chronic phase of infection, *Brucella* only persists in the spleen while being progressively cleared out in other organs, such as the lungs and the liver.

Brucella is known for its ability to escape immunity and particularly detection by the TLRs through different mechanisms. Passive mechanisms involve a modified core and lipid A (Lapaque et al. 2006), and resistance to complement components (Barquero-Calvo et al. 2007). Active mechanisms involve interference with the TLR pathways, through proteins such as Btp1, which modulates microtubular dynamics and interacts with the adaptor MyD88, therefore interfering with the TLR2 and TLR4 pathways (Salcedo et al. 2008; Felix et al. 2014; Sengupta et al. 2010).

After intranasal infection, the total number of CFUs (Colony Forming Units) tends to decrease between 4 and 24 hours post-infection, while the number of bacteria per alveolar macrophage tends to increase over time (Archambaud et al. 2010; Merckx et al. 2016) which leads to the hypothesis that *Brucella* is able to replicate in some cells while being eliminated in others. Studies have identified that the IL-12-dependant and IL-23-dependant IFNγ production is important for immunity against bacterial pathogens (Zabriskie 2009).

Using immuno-deficient mice, it has been showed that $CD8^+$ T cells, $\gamma\delta$ T cells and IL-17RA are linked to *Brucella* control in the lungs, five days after infection, and the the IL-12, the $CD4^+$ T cells and the IFNγ are important for the control at delayed timings (Hanot Mambres et al. 2016). However, the early phase of lung infection remains largely unclear.

Studies have been performed in splenic reservoir cells during the chronic phase of infection by *Brucella,* as the bacteria terminally reach the spleen for settlement. *In situ* analysis of these cells in highly susceptible (IL-12-knockout mice) infected mice demonstrated that they were $CD11c^+CD205^+$ myeloid cells (Hanot Mambres et al. 2015). These cells expressed high levels of arginase1 and were rich in lipids. The arginase1 catalyzes a reaction using L-arginine, which is also used by the nitric oxide synthase (iNOS/NOS1) to produce the anti-microbial NO. The arginase1 therefore depletes the available pool of arginine.

As a result, this suggests that those myeloid cells represent an anti-inflammatory and nutrient-rich environment favoring bacteria persistence (Hanot Mambres et al. 2015). As seen earlier, the T_H1 switch of T_H response is protective against a large panel of pathogens, while a T_H2 profile, as induced for example by allergic asthma, is deleterious for the control of the infection by *Brucella melitensis* (William 2013; Potemberg et al. 2015).

The control of *Brucella* growth in the spleen requires IFNγ -producing $CD4^+$ T cells, involved in the T_H1 response. This has been showed by using MHC II and IFN-γR-deficient mice, displaying a lack of control of the infection (Murphy et al. 2001; Hanot Mambres et al. 2016). The activation and differentiation of those $CD4^+$ T cells requires a functional TLR4/TLR9/MyD88/IL-12 pathway(Copin et al. 2012; Akira & Kiyoshi 2004).

Objectives

Brucella is a representative model of stealth and chronic bacterial infection relying on the ability of *Brucella* to escape immune responses. When the bacteria is settled in the organism, the immune system seems inefficient to get rid of it. Indeed, *Brucella* escapes innate and adaptive immune responses to ensure its survival in a cellular niche. That is why the crucial step both for the organism and *Brucella* is the entry of the bacteria in the body, when *Brucella* and the immune system collide for the first time.

Our objectives for this year will be to characterize the early times of infection by *Brucella melitensis in vivo*. We will mainly investigate the first 24 hours following intranasal infection. Our goals are split in three main axis.

First of all, we will confirm the phenotype of the lungs infected cells as alveolar macrophages with flow cytometry techniques. To achieve this objective, we will use bacteria expressing fluorescent proteins and surface markers antibodies to spot the phenotype of infected cells.

The next goal will be to visualize *Brucella melitensis* growth and division in alveolar macrophages *in situ*, by using membrane labeling allowing us to differentiate newborn cells from the mother cell.

Finally, our third goal will be to determine if immune effectors are able to control the infection during early times after *Brucella* infection in the lungs, by CFUs counting. To perform this identification, we will use knockout mice for key elements of the immune system, and use an allergic asthma model in mice to induce a "T_H2 biased / T_H1-knockout" phenotype that has been shown to favor the growth of *Brucella* by inhibiting the proper immune response.

Materials & Methods

Mice and ethic statements

Mice are purchased from Harlan (Netherlands), bred and raised in the institutional convential animal facility of the Molecular Medicine and Biology Institute of Gosselies (ULB, Belgium). Knockout mice were obtained from the « Université Libre de Bruxelles » (ULB, Belgium). Only mice aged from 6 to 8 weeks were used for the experiments. Mice used are WT (Bicester, U.K.), IFN-$\gamma R^{-/-}$, IL-$12_{p35}^{-/-}$, and IL-$12_{p40}^{-/-}$ (University of Orleans, France), IL-$17R_A^{-/-}$, $MyD88^{-/-}$ and TNF-$R_1^{-/-}$ (Belgian Scientific Institute for Public Health of Bruxelles, Belgium), $CD3^{-/-}$, IL-$1R^{-/-}$, $TCR_{\gamma\delta}^{-/-}$ and $TCR_{\alpha\beta}^{-/-}$ (Bar Harbor, ME), and $TLR_{2,4,9}^{-/-}$ C57Black/6 mice (From Dr. Carsten J. Kirschning ; Institute of Medical Microbiology, University of Duisburg-Essen, Essen, Germany) and WT Balb/C mice. Mice are transferred to the Biosafety level III laboratory facilities of the « Université de Namur » (UNamur, Belgium) one week prior to experimentations.

All procedures abide by European legislation directive 86/609/EEC, and its corresponding Belgian Royal decree regarding animal protection in experimentation (from 2010/04/06, published in 2010/05/14). The complete protocol has been reviewed and approved by the Animal Welfare Committe of the « Université de Namur » (UNamur, Belgium) under the permit number 05-558.

Statistical analysis

The number of mice per group is pre-evaluated to ensure statistical relevance. Data basic treatment are performed with the Microsoft Excel software (Microsoft©) and are subsequently treated for statistical analysis and graphic representation with the GraphPad Prism software (GraphPad Software, inc.). All statistical analysis are performed through the (Wilcoxon-)Mann-Whitney unpaired and non-parametric t test to compare each group of deficient mice with the WT group, or groups with different times of infection (significance levels represented by * when $P<0,05$; ** when $P<0,01$; *** when $P<0,001$). Each dot of the CFUs graphs represents a single organ – single mouse – of its group, while the bar stands for the mean of each group.

Bacteria strain and reagents

The strains used are a WT Nal^R strain of *Brucella melitensis* 16M (Biotype 1 ; ATCC 23456) and a mCherry fluorescent protein stably-expressing (under the control of PsojA, a strong and stable promotor during the *Brucella* spp. cell cycle) Nal^R and Kan^R *Brucella melitensis* 16M (Copin et al. 2012). These strains are conserved at low temperature (-80°C in 30% glycerol solution) in a biosafety level III laboratory facility at the « Université de Namur » (Unamur, Belgium).

$$\frac{OD \times 3.10^9}{V_{ID}\,(mL)} = D$$

$$\frac{V_{TOT}}{D} = V_{Bact}$$

$$V_{TOT} = V_{Bact} + RPMI\,(mL)$$

$OD = 1 = 3.10^9$ bacteria/mL
Vol_{ID} = Infectious dosis Volume (mL)
D = Dilution factor
V_{TOT} = Total Volume (mL)
V_{Bact} = Bacterial solution volume (mL)

Box 1 | Dilution calculation depending on optical densities (OD) of liquid cultures of *Brucella melitensis* at 600λ wavelength.

The bacteria are woken up on 2YT-Agar plates ([32g/L] LB Agar, Invitrogen ; [1g/L] Agar, BD ; [5g/L] Yeast Extract, BD ; [6g/L] Peptone, BD) for a week (incubation at 37°C) and are cultivated in 2YT liquid medium ([32g/L] LB Agar, Invitrogen ; [5g/L] Yeast Extract, BD ; [6g/L] Peptone, BD) overnight at 37°C with shaking. Cultures are done in triplicate.

The cultures in their exponential phase are washed twice (3500g, 10min, 4°C) in RPMI, and are chosen to obtain an OD (optical density) as close as possible of 1 at 600λ. The details of the dilution calculation for the infection dose follow as such **[Box 1]**.

Bacteria Labeling

Cultures of *Brucella melitensis* are centrifuged (3500g, 10min) and washed in PBS (Phosphate-Buffered Saline) at room temperature, three times. Cells are resuspended with TRSE ([1µg/mL] Texas Red Succinimidyl Ester, Invitrogen) or eFluor 670 (eBioscience – ref : 65-0840-85) in PBS, and incubated in the dark for 15 minutes with rotation. The cells are subsequently washed twice in PBS, and once in RPMI for the infection.

Bacteria Stripping

After culture labeling, 1mL is taken (T_0 time) and washed two times with PBS, before being resuspended in 1 mL of paraformaldehyde (2% in PBS). The rest of the culture is washed two times with RPMI and resuspended with liquid 2YT. The culture is put in the incubator for a determined period of time (3, 6, 9, 12 or 24 hours). At the specific timing, 1mL is collected, washed two times with PBS and resuspended with 1mL of paraformaldehyde (2% in PBS).

The fixed bacteria are deposited on a slide with an agarose pad (Agar + PBS), which is sealed with a coverslip and wax. The slides are visualized using a fluorescence microscope in the BL3 facility.

Mice Infection & Euthanasia

Mice are anesthetized by intraperitoneal injection of a cocktail of Xylazine (460µL/Kg Xyl-M 2% ; VMD – ref :00115.02) and Ketamine (720µL/Kg Ketamine 1000 ; Ceva – ref : 804119) in cold PBS (16mL/Kg). Mice are then inoculated intranasally with *Brucella melitensis* 16M mCherry or WT for the infection, with a high dose of 2.10^7 CFUs (for histology and flow cytometry protocols) or a low dose of 2.10^4 CFUs (in 30µL of RPMI).

Control mice are inoculated with the same volume of RPMI. The infectious doses are also plated on 2YT Agar medium plates under serial dilutions as control.

Mice are sacrificed at a defined time (4h, 24h) by cervical dislocation and are immediatly prepared for the bacterial count protocol, the flow cytometry protocol, or the microscope analysis protocol.

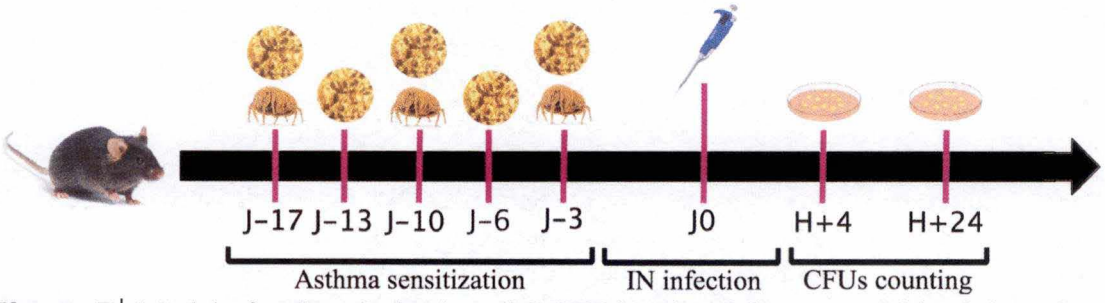

Figure 7 | Model of asthma induction of C57BL/6 mice. Mice are sensitized three times with House Dust Mite (HDM) extract once a week, or five times with *Alternaria alternata* before infection. Mice are then sacrificied 4 hours or 24 hours after infection for CFUs counting.

Mice dissection

Euthanized mice are placed on their right side under the hood, and are sprayed with 70% ethanol for asepsis. The side skin is removed with scissors and the exposed peritoneum is also sprayed with ethanol before cut open. The organs needed for the protocol are then removed (entire lung or one lobe).

Induction of allergic asthma

Mice are placed one by one in a box containing gazeous Isoflurane (Abbott laboratories, n°B506 ; 1mL for 5 mice) until fainting, and are subsequently injected intranasally with HDM (*Dermatophagoides farinae*) extract(*) (100µg in 50µL of PBS) or *Alternaria alternata* extract (5µg in 100µL of PBS; Belgian Scientific Institute for Public Health of Bruxelles, Belgium).

Injections of HDM are realised on days -17, -10 and -3 before intranasal infection with *Brucella melitensis* (one resting week between each injection), while Alternaria alternata injections are realized on days -17, -13, -10, -6, and -3 before infection (twice a week before infection), following the model of induction already described by Fabrice Bureau (Marichal et al. 2010) **[Figure 7]**.

Bacterial count

Organs are weighed and crushed in sterile plastic bags (VWR® International) then resuspended in 1mL of PBS/0,1% X-100 Triton(*) (VWR® – ref :28817.295). For experiments using knockout mice, 100µL (10^0 dilution) or 10µL (10^{-1} dilution) of the resuspension are plated on 2YT Agar + Kanamycin medium plates. For experiments using asthmatic mice, serial dilutions are done in a 96 wells plate (In RPMI), and the 10^{-3} and 10^{-4} dilutions are plated. Plates are left at 37°C for 5 days before CFUs (Colony forming units) counting.

Flow cytometry analysis

Lungs are placed in 6 wells plate and are dampened with two drops of a mix of CollagenaseD(*) ([4000U/mL] ; Roche) and DNAse(*) ([10mg/L] ; Sigma) in RPMI. The organs are then torn apart with scissors and resuspended in 1mL of the CollagenaseD/DNAse(*) mix. The plates are left at 37°C for incubation (1 hour, 5% CO2, with incline) and 7 mL of cold RPMI are added to each well. With a 1mL syringue, the content is sucked up and spat out against the surface of the well about twenty times to shear the remaining tissue. The content is then filtered using a bridal veil (pores of 70µm) and the filtrate is collected in a 15mL tube (Corning® CentriStar™). The tubes are then centrifuged (1400rpm ; 7min ; 4°C).

(*) See « Media & Reagents »

SURFACE ANTIBODY	CHANEL	DILUTION	REFERENCE
SiglecF	APC	1/200	BD Pharmigen – ref : 55126
CD11b	FITC	1/200	BD Pharmigen – ref : 553310
CD11c	PE	1/200	BD Pharmigen – ref : 553802
F4/80	APC	1/200	eBioscience – ref : 17-4801-82
Ly6G	FITC	1/400	BD Pharmigen – ref : 551460
24G2 (CD16/CD32)	/	1/200	BD Pharmigen – ref : 553142

Table 4 | List of surface antibodies used for flow cytometry protocols and their chanel of detection.

Immuno-Phenotyping	CD11b	CD11c	Ly6G	F4/80	Siglec F
Alveolar Macrophages	$+_{med}$	$+_{high}$	-	+	+
Dendritic cells	+	+	+	-	-
Neutrophils	$+_{high}$	-	$+_{high}$	-	-
Eosinophils		-		+	+

Table 5 | Cellular types and their associated surface markers.

[If intracellular staining, the cells are resuspended in a mix of completed RPMI(*) (5mL) and the protein transport inhibitor BD Golgi Stop (1/1000 ; BD Biosciences – ref : 51-2092KZ). The tubes are incubated with unscrewed cap for approximatively 5 hours (37°C ; 5% CO2). The tubes are then centrifuged (1400rpm ; 7min ; 4°C), resuspended in 1mL of completed RPMI(*), and left over night at 4°C. The day after, the tubes are centrifuged (1400rpm ; 7min ; 4°C).]

The supernatent is thrown away and the cells are resuspended in 200µL of FACS-Buffer ([2g/L] BSA ; [0,2g/L] NaN_3 azide ; PBS under agitation), 150µL of which are added to a 96 wells plate. The plate is centrifuged (2000rpm ;1min45''), resuspended in a mix of FACS-buffer, Rat serum ([1/200]) and anti-Fc antibody 24G2 ([1/200]), and kept at 4°C for 20 minutes.

The plate is centrifuged again (2000rpm ;1min45''), resuspended with 195µL the proper surface antibody mix ([1/200] diluted in cold FACS-Buffer) and kept at 4°C for 30 minutes **[Table 4]**. The plate is centrifuged for the third time (2000rpm ;1min45'') and the the supernatent is replaced by FACS-Buffer. This last operation is done two more times. The cells are then resuspended in 150µL of paraformaldehyde 1% diluted in FACS-Buffer, and kept at 4°C for 15 minutes.

[If intracellular staining, the plate is then centrifuged (2000rpm ; 1min45'') and the supernatant is replaced by FACS-Buffer, three times. The cells are resuspended in 150µL of a mix containing the intracellular antibodies and Permwash (10% ; BD Biosciences – ref : 51-2091KZ) diluted in FACS-Buffer, and kept at 4°C for 30 minutes.]

The plate is centrifuged (2000rpm ; 1min45'') and the supernatant is replaced by FACS-Buffer, three times. The cells are then resuspended in 150µL of FACS-Buffer, and transferred into FACS tubes (1mL) already filled with 400µL of paraformaldehyde 1%.

Samples are analysed with the BD FACSVerse™ (BD Biosciences) flow cytometer. The combination of surface markers is informative about the cellular type of infected cells positive for the TRSE signal (mCherry) or APC signal (eFluor670) **[Table 5]**.

Fluorescence microscopy

The organs are placed in 15mL tubes filled with paraformaldehyde 2%, and kept in the dark at room temperature for 2 hours. The organs are then washed two times with PBS, and immerged in a 20% sucrose solution ([0,2g/mL] D(+)-Saccharose ; VWR Chemicals – ref : 27483.294 ; in PBS). The tubes are left at 4°C over night. The supernatant is removed and the organs are washed in PBS. They are then diagonally placed in plastic cryomolds (VWR® - ref : 25608-92) containing O.C.T (Tissue-Tek® O.C.T.™ ; Sakura® - ref : 4583) for 10 minutes. The cups are cooled off with liquid nitrogen and the O.C.T is solidified. The cups are then kept in dry ice until the cutting in the cryostat chamber. Slices 5µm thin are cut off and laid on microscope slides (SuperFrost® Plus ; VWR® - ref : 631-0108). The slides are kept at -20°C.

(*) See « Media & Reagents »

The slides are then hydrated with cold PBS for 10 minutes, and a pool of PBS is delimited to prevent the organ from drought. 200µL of PBS-BR 1% are added for the blocking of non-specific sites, and slides are left for incubation 20 minutes at room temperature. The slides are then washed several times with cold PBS and a pool is then again delimited. 200µL of diluted markers/antibodies in PBS-BR 1% are added and the slides are left overnight in a humid box at 4°C.

The slides are washed several times in successive bath of cold PBS, and a pool of PBS is delimited on the slides. 200µL of the secondary antibodies diluted in PBS-BR 1% are added, and the slides are left for incubation 2 hours at 4°C. They are then washed several times in successive bath of cold PBS. The cover slip is added on top of the slide with FluoroGel medium (Electron microscopy Sciences – ref : 1785-10). The slides are now ready for microscope analysis.

Macrophages culture

The cryotube (1mL, -80°C) containing the RAW 264.7 macrophages is quickly melted in a 37°C bath, due to the toxic DMSO (dimethyl sulfoxide) exposure to macrophages. The content is directly transferred in a 50mL Falcon (Corning® 50 mL centrifuge tubes - CLS4558 SIGMA) containing 9mL of DMEM culture medium (DMEM without pyruvate ; Glucose [4,5g/L] ; decomplemented FCS 10% - 56°C for 30 minutes ; Non-essential amino acids 1% ; L-glutamine 1%) at 37°C.

The tube is centrifuged at room temperature, 1200rpm for 10 minutes. The supernatent is removed and the cells are resuspended with 1mL of DMEM medium at 37°C, before being transfered into a T75 flask (75cm² Corning® CellBIND Flask) containing 19mL of DMEM medium at 37°C. The cells are distributed in the medium by gently shaking the flask, which is left for incubation at 37°C with 5% CO2.

Macrophage passage

When the macrophages reach approximatively 80% of confluence, the DMEM medium is removed from the T75 flask. 20mL of sterile PBS at 37°C are added to wash the surface of the flask. The cell layer is gently scraped with a sterile rake to detach the macrophages. The suspension is transferred into a 50mL falcon and centrifuged for 10 minutes at room temperature 1200rpm.

The supernatant is removed, and the cells are resuspended with 1mL of DMEM medium at 37°C. Depending on the dilutions, 50 to 100 µL are collected and added to a new T75 already containing 20mL of DMEM medium at 37°C. The cells are distributed in the medium by gently shaking the flask, which is left for incubation at 37°C with 5% CO2.

Preparation of macrophages-containing plaques

The DMEM medium is removed from the T75 flask containing the adherent macrophages. 20mL of sterile PBS at 37°C are added to wash the surface of the flask. The cell layer is gently scraped with a sterile rake to detach the macrophages. The suspension is transferred into a 50mL falcon and centrifuged for 10 minutes at room temperature 1200rpm. The supernatant is removed, and the cells are resuspended with 1mL of DMEM medium at 37°C.

The cell concentration is assessed by using a Neubauer chamber. 10 µL of the cellular suspension are injected in the chamber, as well as 10 µL of Trypan blue to differentiate live from dead cells. The four squares of the chamber are counted. The calculation follows as such:

Mean of the 4 squares X 2 (dilution due to Trypan blue) X 10.000 = Nb Cells/mL

In order to have a cellular density approaching 4.10^4 after 24 hours, 2.10^4 have to be added in each well. 500 µL of the proper dilution (in DMEM medium) are added in each well. Each condition and timing are represented by 3 or 4 wells for biological replicates.

Macrophages activation

If a condition needs the macrophages to be activated, the activation is done 7 hours after the preparation of the plaques, in order to avoid an excess of stress for the macrophages. The medium is removed from the wells and replaced by LPS/IFNγ medium (DMEM medium; LPS [2mg/mL]; IFNγ [10µg/50µL]). The activation medium is left until the day after (day of infection).

Macrophages infection

The infectious dose is prepared in order to have approximately 100 bacteria per macrophage (4.10^6 bacteria per well). For non-activated macrophages, the dose of eFluor670-labeled mCherry-expressing *B. melitensis* is made in DMEM medium. For activated macrophages, the dose is prepared in LPS/IFNγ medium to keep the macrophages activated. The infectious dose is smeared on 2YT agar plate as a control.

The supernatant of the plaque is removed, and the infection medium is added. The plaque is centrifuged (1000rpm, 10min, 4°C) in order to put the bacteria in contact with the macrophages. The plaque is then left for incubation for 1 hour (37°C), which represents our T_0 timing.

The wells are gently rinsed with PBS at 37°C. The PBS is then removed and replaced with gentamycin medium (Gentamycin [50mg/mL]) to eliminates the excess of bacteria. This medium is left in the wells until the end of the experiment.

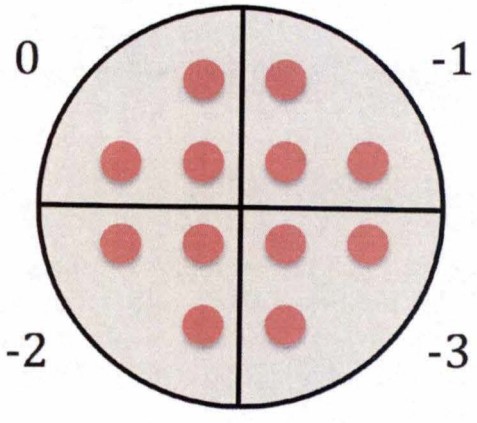

Figure 8 | Disposition of the CFUs drops on the 2YT Agar plate

Macrophages CFUs counting

At the specific timing, the medium is removed from the well, and the cells are rinsed with PBS. PBS-Triton (0,1%) is added to lyse the cells, and the wells are flushed a determined number of times (for exemple 15 times) to standardize the procedure. The plaque is left for incubation for 10 minutes (37°C) to allow the Triton to act.

Serial dilutions (10^0, 10^{-1}, 10^{-2}, 10^{-3}) are made for each well in PBS. Three drops of 20µL of each dilution (for technical replicates) are deposited on a quarter of a 2YT Agar plate **[Figure 8]**.

Media & Reagents

PBS 10x : NaCl [80g/L], KCl [2g/L], Na2HPO4 [11,5g/L] and KH2PO4 [2,4g/L] are dissolved in bidistillated water under agitation at room temperature. The pH is set to 7,4.

PBS-0,1% Triton : 1mL of Triton is added in 1L of PBS 1x and the solution is autoclaved. Regarding the viscosity of Triton, the tip is widen with scissors.

HDM extract : Lyophilized House Dust Mites (*Dermatophagoides farinae*) were obtained from Greer Laboratories (Lenoir, NC ; [0,84ng/mg] endotoxin).

Completed RPMI : 500mL of RPMI are completed with 50mL of decomplemented FBS (57°C, 30 minutes ; Invitrogen – ref : 10270-106), 5mL of L-Glutamin (Life technologies – ref : 25030-024), 5mL of non-essential amino acids (Life technologies – ref : 11140-035), 5mL of Pyruvate sodium (Life technologies – ref : 11360-039) and Gentamycin ([50mg/mL]). The medium is stored at 4°C.

Collagenase (4000U/mL) : Lyophilized collagenase D (Roche – ref : 11088866001) is resuspended in non-sterile RPMI in order to obtain 4000U/mL. The solution is then aliquoted (1mL) in Ependorf.

DNAse : Lyophilized DNAse (Deoxyribonuclease I from bovine pancreas ; Sigma – ref :D4513) is resuspended in autoclaved NaCl solution ([0,15M]) to obtain a concentration of [10mg/mL]. The solution is then aliquoted (100µL) in Ependorf.

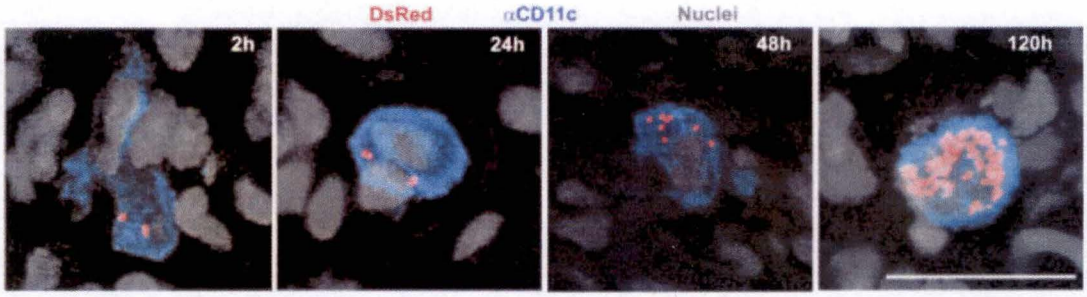

Figure 9: Infected lungs cells 2, 24, 48 and 120 hours after intranasal infection with *B. abortus* (red) (Archambaud et al. 2010). The inoculation dose is 5.10^5 CFUs. The infected cells are CD11c-positive (blue),suggesting they might be alveolar macrophages. Nuclei are represented in grey.

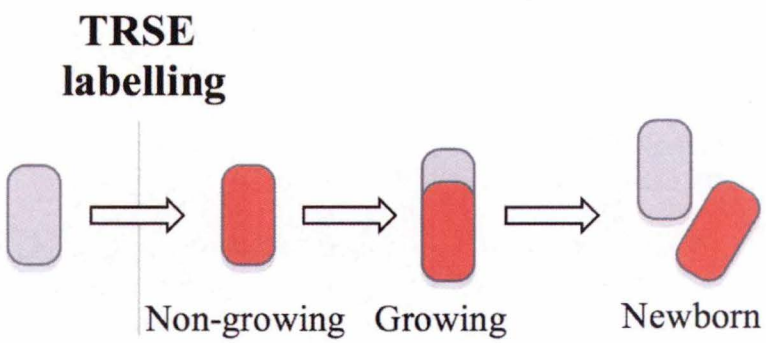

Figure 10: Distinction between newborn and mother cells by using TRSE membrane labeling (Merckx et al. 2016).

Results

I. Phenotyping of infected cells

Studies led by Archambaud showed that after intranasal inoculation of 5.10^5 bacteria in mice, *B. abortus* firstly infects CD11c-positive, CD11b-positive, F4/80-positive cells with high auto fluorescence, and strive in those cells **[Figure 9].** This phenotype suggests that infected cells were alveolar macrophages (Vermaelen & Pauwels 2004; Archambaud et al. 2010). However, if the alveolar macrophages population was depleted, bacteria were also found in DCs (CD11c-high, CD11b-low, MHC II-high) (Archambaud et al. 2010). Globally, based on these results, the authors suggest that following intranasal infection, *Brucella* preferentially infects alveolar macrophages before its dissemination to lower organs (von Bargen et al. 2012; Archambaud et al. 2010).

We have previously generated a strain of *Brucella melitensis*, stably expressing the mCherry fluorescent protein (derived from the *Actinodiscus* coral) (Copin et al. 2012). This fluorescent strain allow the detection of infected cells *in situ* by microscopy but only following infection with an high dose of bacteria (2.10^7 CFUs). At lower doses, the frequency of infected cells is too low to allow the observation of infected cells *in situ*. Flow cytometry analysis allows the monitoring of a great number of cells in a short period of time. Unfortunately, the intensity of mCherry expression by infected cells does not allow its detection during the first time of infection where a few number of bacteria are contained in infected cells (data not shown). To solve this problem, we tried to develop a protocol to stain the membrane of bacteria with a highly bright fluorochrome.

I.1. Use of eFluor670 for *Brucella* detection

In his paper of 2014 (Deghelt et al. 2014), Deghelt used a membrane-targeting dye to label *Brucella*. This dye is the TRSE (Texas Red Succinimidyl Ester) which reacts with primary amines of the outer membrane proteins and forms covalent bond (Hoefel et al. 2003). The fluorophore (Texas Red) emits in 615 nm wavelengths. This was used in order to monitor *Brucella* cell division in vitro in HeLa cells (Deghelt et al. 2014) and in RAW 264.7 macrophages (Merckx et al. 2016). Indeed, as *Brucella* displays an atypical unipolar growth and the proteins are anchored to the peptidoglycan, thus displaying no motion, TRSE-labeled bacteria spawn new unlabeled, or partially labeled cells, allowing the distinction between mother cell and newborn ones [**Figure 10**]. Deghelt also used, in addition to the TRSE, a LPS-staining to detect all bacteria, including the TRSE unlabeled newborn ones (Deghelt et al. 2014).

However, the LPS staining used previously has the disadvantage of labeling all bacteria, whether they are dead or alive. This might be a huge drawback when it comes to study bacterial cell cycle *in vivo*. The mCherry-expressing *B. melitensis* strain offers an alternative, as its constitutive fluorescence allows distinction between membrane-labeled bacteria – mother cells – and unlabeled mCherry-expressing bacteria – newborn cells.

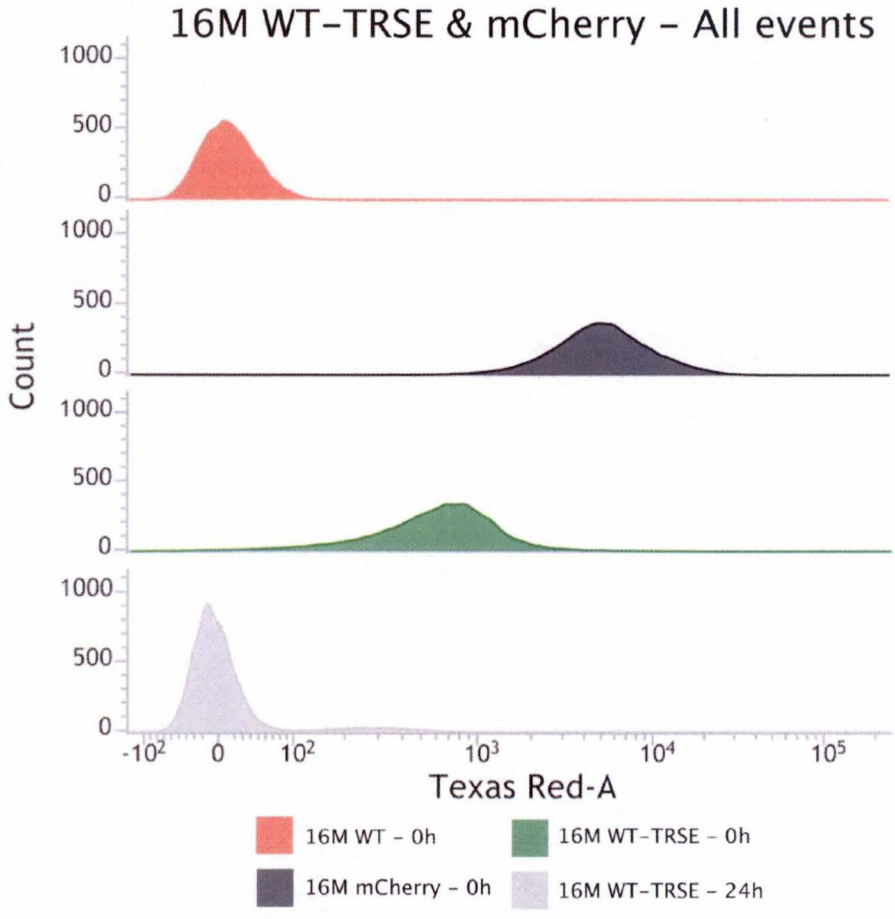

Figure 11: Flow cytometry analysis of the emission spectrum (in the Texas Red-A chanel) of TRSE-labeled WT *B. melitensis* (green), unlabeled WT *B. melitensis* (red) and mCherry-expressing *B. melitensis* (black). The analysis is also performed on the WT strain labeled with TRSE 24 hours prior to the analysis (grey).

In addition, the expression of mCherry is aborted and the protein degraded after the death of the bacteria, which excludes false positives.

Limits of Succinimidyl Ester-coupled fluorochromes for Brucella detection in vivo

We tested the TRSE labeling in order to see if it was an interesting tool to monitor cell growth, in addition to our mCherry-expressing *B. melitensis*. We performed flow cytometry analysis on bacteria samples composed of the WT strain of *B. melitensis* labeled with TRSE, the WT strain alone and the mCherry-expressing strain alone. We also made the TRSE labeling on the WT strain 24 hours prior to the analysis to see if the TRSE signal was strong enough to be detectable after such time.

The results enlightened few problems with the TRSE labeling **[Figure 11]**. First of all, the TRSE and the mCherry emission signals are overlapping in the Texas Red-A channel. This is a significant problem to differentiate TRSE-positive mCherry-expressing and TRSE-negative mCherry-expressing cells. Secondly, the intensity of the TRSE signal is one Log weaker than the mCherry signal. Even though this problem might be bypassed by using higher doses of TRSE, this might be detrimental to histology analysis. Finally, the TRSE signal is completely lost after 24 hours, making it useless to detect labeled bacteria (mother cell) past that time.

We also tested another membrane labeling by using the APC-SE (allophycocyanin succinimidyl ester). Due to the SE, the APC binds to the primary amines of the outer membrane protein, similarly to the TRSE. Moreover, the emission spectrum of the APC is around the 660nm, making it easily distinguishable of the TRSE and mCherry signal. However, despite the use of several buffers to improve APC labeling, the dye does not seem to bind to *B. melitensis* anyhow under our conditions (data not shown).

Development of eFluor670 as a new tool for Brucella detection

The use of a dye that was emitting in the APC-A channel was the perfect way to distinguish the membrane labeling and the constitutive signal. The tool to fulfill this objective was quickly brought to us.

The eFluor® 670 (eBiosciences™) is a cell proliferation dye that is usually used to monitor eukaryotic cells divisions. It has however the particularity to bind to any primary amines, which includes the amines of the bacteria outer membrane proteins. This dye emits at 670 nm wavelengths, which make it also detectable in the APC-A channel.

We made the same experiment with, this time, the eFluor 670 labeling. However, in order to see if it was the proper tool to be used on the mCherry-expressing *B. melitensis*, we only labeled this fluorescent strain. The WT strain and the mCherry strain alone were used as controls. We also did a 24 hours incubation time in RPMI at 37°C to assess the loss of the signal.

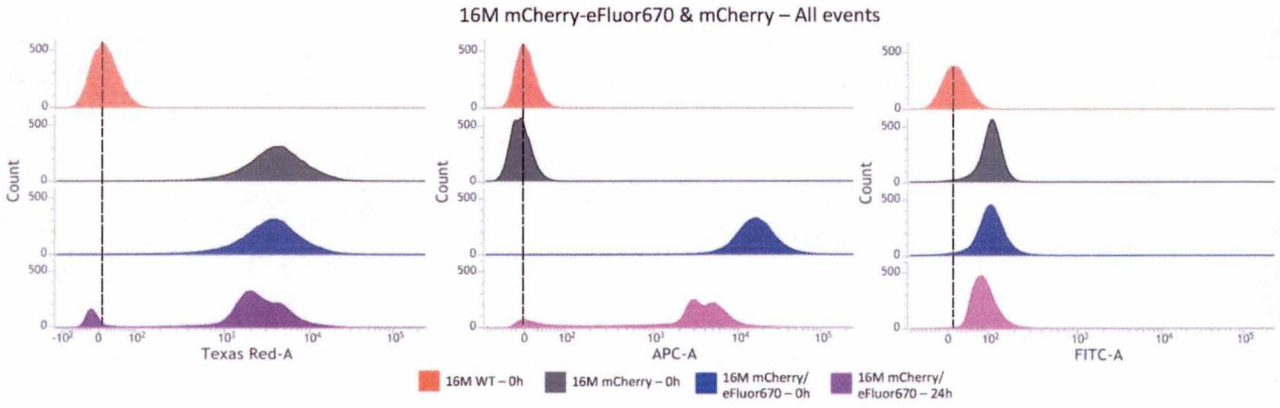

Figure 12: Flow cytometry analysis of WT *B. melitensis* (red), mCherry-expressing *B. melitensis* (black), and eFluor 670-labeled mCherry-expressing *B. melitensis*, right after labeling (blue) or after 24 hours of incubation (purple) in liquid 2YT cultures, according to the signal intensity in the fluorescence channel. The analysis has been performed in three different channels of fluorescence, the Texas Red-A, the APC-A and the FITC-A channel.

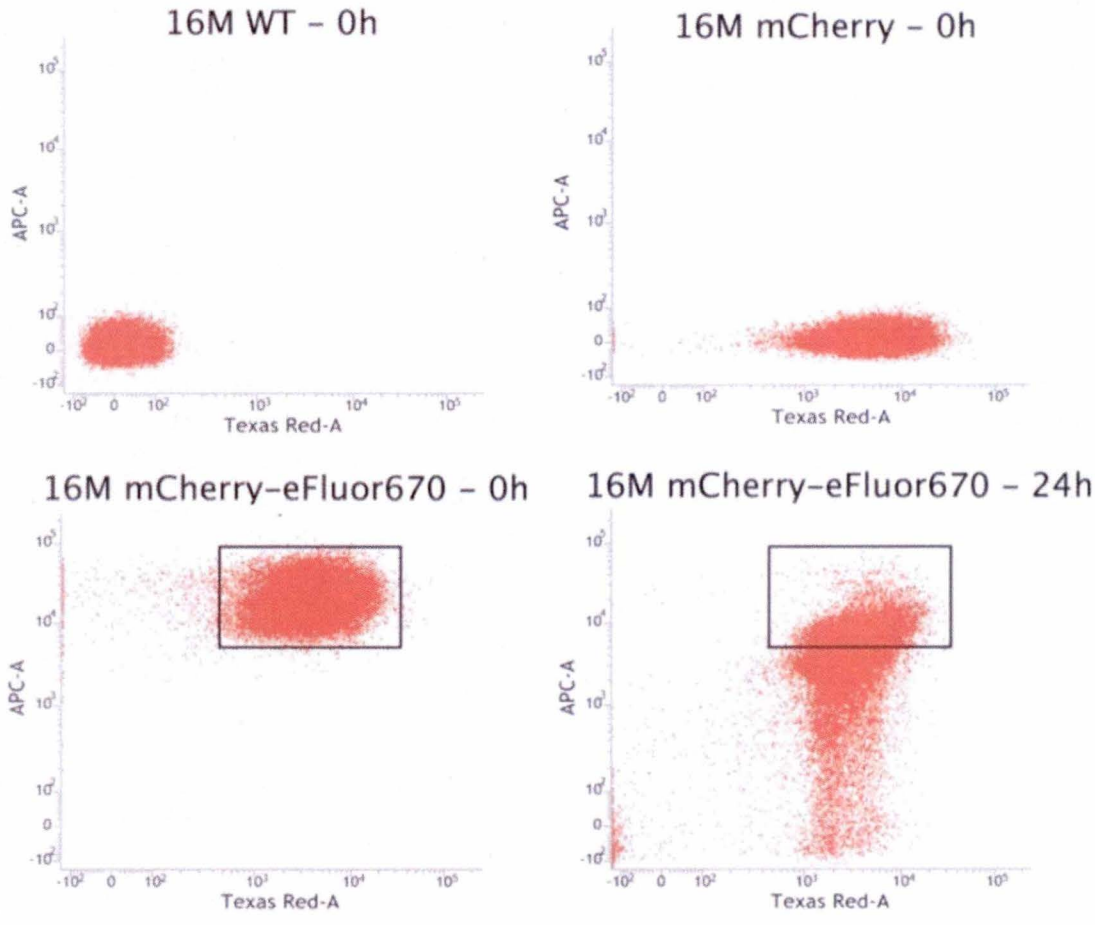

Figure 13: Flow cytometry analysis of WT *B. melitensis*, mCherry-expressing *B. melitensis*, and eFluor 670-labeled mCherry-expressing *B. melitensis*, right after labeling or after 24 hours of incubation in liquid 2YT cultures, according to their respective signal intensities in the APC-A and Texas Red-A channels.

We analyzed the fluorescence linked to the mCherry protein and the eFluor 670 label in three different channels: the Texas Red-A, the APC-A and the FITC-A channels [**Figure 12**]. As expected, the WT control *B. melitensis* is negative for any fluorescence signal detectable in our three channels. The mCherry-expressing strain is positive for a Texas Red signal, which is also slightly detectable in the FITC-A channel.

If we focus on the eFluor 670-labeled mCherry-expressing strain, we can see that the signal is not distinguishable of the mCherry strain in the Texas Red-A. That is not surprising as the labeled bacteria express the same mCherry protein as the unlabeled ones. However if we take a look in the APC-A channel, we can see that while the mCherry strain is not detectable in this channel, the membrane labeling is visualizable and strongly differentiated from the mCherry/TRSE signal.

Moreover, the signal shows only a slight decrease of intensity of approximately half a Log after 24 hours of labeling, which means that the eFluor 670 is a relevant tool to assess *Brucella* detection during the first 24 hours. But we had to know if this label allowed us to assess *Brucella* replication, similarly to the TRSE, and to detect the stages of bacterial growth and division (Merckx et al. 2016).

To do this, we analyzed the flow cytometry samples according to their APC-A (the eFluor 670 membrane labeling) and Texas Red-A (the mCherry protein) signals [**Figure 13**]. As expected, the WT *B. melitensis* is concentrated in a spot negative both for TRSE and APC signals. The mCherry strain is negative for the APC signal, and positive for the Texas Red-A signal. The interesting part is that at 0 hours post-labeling, the eFluor 670-labeled mCherry *Brucella* is concentrated in an area positive both for Texas Red-A and APC signals.

After 24 hours, we can observe a smear of cells with basically the same intensity of signal for the Texas Red-A, but with a heterogeneous range of intensity for the APC/eFluor 670 signal, which might represent a mixture of non-growing or non-dividing bacteria (APC-positive), newborn bacteria (APC-negative) and growing or dividing bacteria (intermediate). We can also see the loss of intensity of the signal of half a Log as seen in Figure 12. We can also spot a small but disconcerting APC-negative and Texas Red-A-negative population that might be composed of bacterial debris. We also analyzed a mix, after fixation, of eFluor 670-labeled bacteria and non-labeled bacteria to see if the eFluor 670 was able to spread and dye other bacteria even after fixation. However, the results showed two specific and segregated populations, leading us to think that the dye was not transferred from a cell to another (data not shown).

Now that the eFluor 670 labeling has been performed on *B. melitensis* cultures, the next step is to visualize the bacteria division after infection, *in vivo* in mice alveolar macrophages, or *in vitro* in RAW 264.7 macrophages.

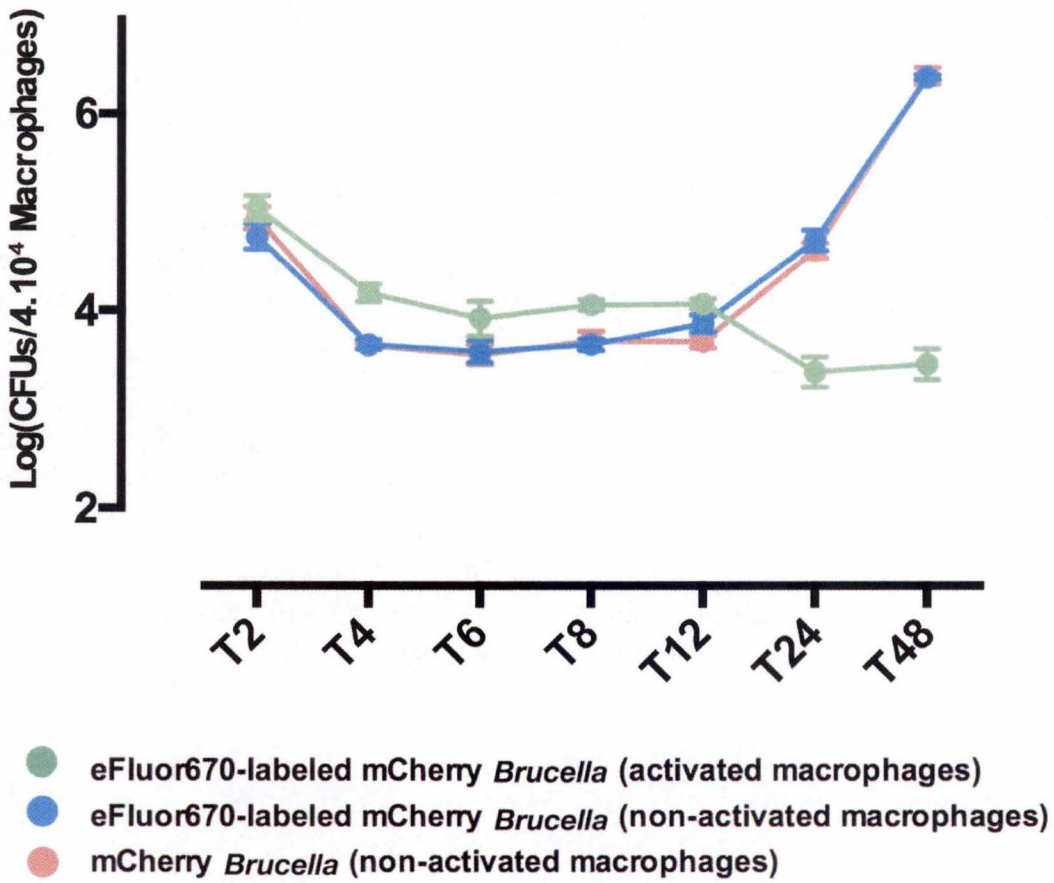

Figure 14 : Colony forming units (CFUs) analysis *in vitro* of infected non-activated RAW 264.7 macrophages with mCherry-expressing *B. melitensis* (red) and eFluor 670-labeled mCherry-expressing *B. melitensis* (blue), and infected LPS/IFNγ-activated RAW 264.7 marophages with eFluor 670-labeled mCherry-expressing *B. melitensis*, 2 hours, 4 hours, 6 hours, 8 hours, 12 hours, 24 hours and 48 hours post-infection. Kinetics profile of labeled and non-labeled *Brucella* are highly similar in non-activated macrophages.

II. Visualization of *Brucella* growth and division *in vivo* using eFluor 670

Our objectives are the phenotyping of the infected cells and the monitoring of *Brucella melitensis* growth and division using a proper membrane labeling, during the course of infection *in vivo*. To address these issues, we used two main techniques.

The first one is, once again, flow cytometry. This time, flow cytometry analysis will allow us to detect lungs cells positive for a fluorescence signal, and not directly labeled bacteria. Let us remember that after division, the newborn cells will acquire no or little membrane labeling, while the mother cell will keep most of. Therefore, the use of an eFluor 670-labeled mCherry-expressing *Brucella* will have three consequences:

- There will be no synthesis of eFluor 670 proteins by *Brucella*. Thus, the global pool of eFluor 670 in the infected cells will remain stable until the elimination of the bacteria. This signal will therefore not show any increasing with the multiplication of bacteria inside the cell.
- The mCherry is actually stably synthetized by *Brucella*, so the intensity of the mCherry signal inside the host cell will proportionnally increase with the number of replicating bacteria.
- The global pool of mCherry protein will increase after division in a determined infected cell, as more bacteria will be present to synthetize the protein.

We thus expect that, as time goes by, the intensity of the mCherry signal will increase while the eFluor 670 signal will globally stay still.

The second technique used to fulfill our objective is fluorescence microscopy, which represents a more visual and concrete method to assess *Brucella* division. This technique might be performed on cultures of bacteria, but also on lungs tissue to monitor cell division *in vivo*.

II.1. Absence of impact of eFluor670 labeling on CFUs *in vitro*

First of all, before engaging in further experiments, performing infections, investigating flow cytometry analysis, producing data and drawing conclusions out of it, one could wonder if we did not introduce a huge bias by labeling the mCherry-expressing *Brucella* with eFluor 670. Indeed, we can imagine that the bacteria, burdened by those molecules would be less apt to perform an efficient infection, or that it would be more easily recognizable by the immune system, the eFluor 670 hiding some PAMPs of the bacteria. Moreover, we simply cannot afford ourselves to label all the bacteria used for infection in CFUs investigations we will describe later, due to the number of experiments we repeatedly performed.

However, we performed CFUs counting at times 2, 4, 6, 8, 12, 24 and 48 hours following *in vitro* infection on RAW 264.7 macrophages, with eFluor 670-labeled and unlabeled mCherry-expressing *Brucella* in non-activated macrophages **[Figure 14]**. The results showed that the two CFUs curves display striking similarities, suggesting that the

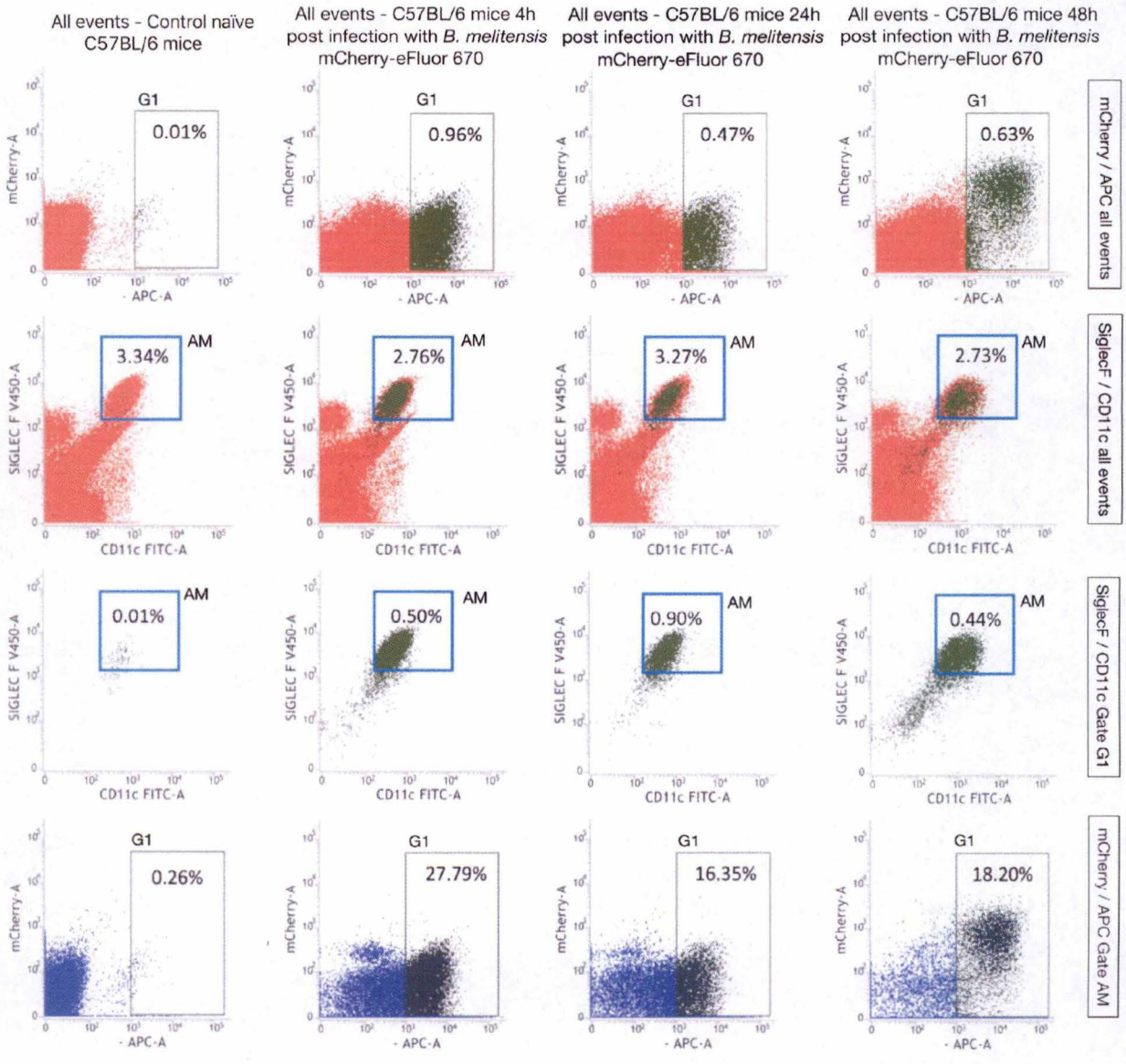

Figure 15: Flow cytometry analysis of (all events) lungs cell population in control C57BL/6 mice (first column), and in infected mice with eFluor670-labeled mCherry-expressing *B. melitensis*, 4 hours (second column), 24 hours (third column) and 48 hours (fourth column) after infection. Cells are distributed according to their mCherry/Texas Red-A signal and their eFluor670/APC-A signal (first row). The gate G1 is set arbitrarily to define cells negative for eFluor670 signal in WT mice. The cells are also distributed according to their SiglecF and CD11c membrane markers, in all events (second row) or in the gate G1 (third row). The gate AM is put to define the alveolar macrophages population. Cells included in the AM gate are then distributed according to their mCherry/Texas Red-A signal and their eFluor670/APC-A signal (fourth row). The G1 gate is also displayed to visualize alveolar macrophages positive cells.

eFluor 670 labeling have no impact on the course of infection by *B. melitensis* in RAW 264.7 macrophages.

We also infected LPS/IFNγ-activated RAW 264.7 macrophages with eFluor-labeled mCherry-expressing *Brucella* to match with what has already been done by Merckx (Merckx et al. 2016) and see if the macrophage itself was able to control the infection **[Figure 14]**. The results showed that the CFUs tend to decrease over time until 48 hours, suggesting that activated macrophages are able to partially control the infection. We can also see a slight increase of the CFUs number for the 12 first hours when compared to non-activated macrophages. This might be explained by the active uptake of the bacteria by activated macrophages during infection.

II.2. Visualisation of *Brucella*-infected cells in lungs from infected mice by flow cytometry

We used C57BL/6 mice that were classified into four groups. The first one was the control group, with naïve uninfected mice. The other three groups were mice infected with the eFluor 670-labeled mCherry-expressing *B. melitensis* at high doses (2.10^7 CFUs) 4, 24 and 48 hours prior to the analysis. The data presented show representative dot plot (mCherry/TRSE and eFluor 670/APC signal) from individual lung **[Figure 15]**.

Similarly to previous flow cytometry analysis, we displayed a gate (G1) in the control sample (naïve mice) in an area that was negative for the eFluor 670 signal. The same gate G1 has been applied to the other samples.

We used two surface antibodies to phenotype the infected cells. We used an anti-CD11c, a marker found on alveolar macrophages and DCs as previously used, but also an anti-SiglecF. The latter is present on the surface of eosinophils and alveolar macrophages, but not on the surface of DCs and neutrophils. The population of interest, namely the alveolar macrophages, would therefore be CD11c-positive and SiglecF-positive.

The cells were distributed according to their membrane surface markers, and the gate AM, which delimits the alveolar macrophages population, has been displayed. We can see that the major proportion of positive cells is situated in the AM gate, which suggests that the infected cells are alveolar macrophages as expected.

Gated on AM, we redistributed the cells according to their APC and mCherry signals, to focus on what was happening in the population of interest. The gate G1 has been applied to detect positive cells for the eFluor 670/APC signal. We can see that 4 hours after infection, APC-positive cells appear in the gate G1 although the mCherry signal oddly seems to be as intense as the background signal.

At 24 hours after infection, we can see that there are practically two times less positive cells in the G1 gate, but the intensity of the signal for both mCherry and eFluor 670 remains steady. This might be explained by a partial control of the infection by the immune system, resulting in a decreasing overall number of bacteria in the lungs.

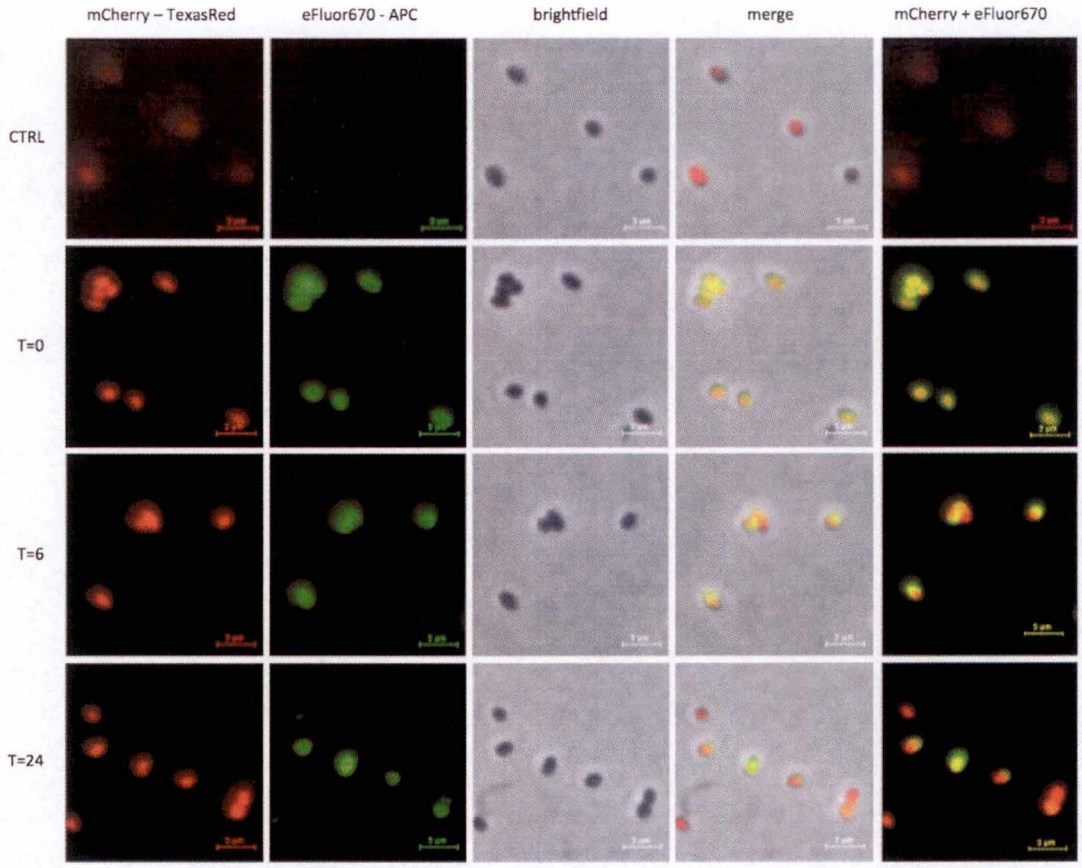

Figure 16: Visualization of *Brucella* growth and division *in vitro* by fluorescence microscopy on *B. melitensis* liquid 2YT cultures. Non-labeled mCherry-expressing *B. melitensis* were used for control. eFluor 670-labeled mCherry-expressing *B. melitensis* were visualized right after labeling (T=0), 6 hours (T=6) and 24 hours (T=24) after labeling.

However, if you take a look at 48 hours post infection, you can see that, first of all, the number of positive cells is slightly increasing, but also that the mCherry signal seems to strongly increase as well while the eFluor 670 signal remains stable. As previously explained, this might be explained by *Brucella* divisions inside infected cells as the mCherry protein is newly synthesized by newborn bacteria while the global pool of eFluor 670 per cell stays unchanged.

This surprising result leads us to conclude that while the immune system is able to have a partial control of the infection, the remaining bacteria are able to strive and actively proliferate in alveolar macrophages.

II.3. Visualization of *Brucella* growth and division *in vitro* by fluorescence microscopy

We analyze in kinetics (0 hours, 6 hours and 24 hours post-labeling) the expression of eFluor 670 signal on mCherry-expressing *Brucella in vitro* [**Figure 16**]. We used the mCherry-expressing *B. melitensis* alone as a control. Due to circumstances we cannot explain, the mCherry signal was a bit weaker, although detectable, than in the other samples.

At time 0 hours post labeling, we can still observe the perfect colocalization between the mCherry and the eFluor 670 signals, and the membrane-specific labeling of the eFluor 670.

At time 6 hours post infection, we can see that the bacteria are mostly labeled on half of the membrane, which leads us to think that the difference "labeled mother cells / unlabeled daughter cells" might be a little bit more complex than this simplistic dichotomy.

At time 24 hours post labeling, we can observe heterogeneity in the membrane labeling, with entirely labeled *Brucella*, which might represent non-growing bacteria rather than mother cells, half-labeled and non-labeled bacteria.

However, we can easily imagine that statistically, even if the eFluor 670 is transmitted in small proportions to daughter cells, following successive division, daughter cells will be more likely to acquire no membrane labeling. Consequently, the *Brucella* with the most membrane labeling would be more likely to be the original mother cell.

We also wanted to visualize *Brucella* division during *in vitro* infection on RAW 264.7 macrophages before performing *in vivo* infections. However, due to reasons we cannot explain, the obtained results for this part were incomprehensible and unusable (data not shown). This experiment still remains to be repeated at this time.

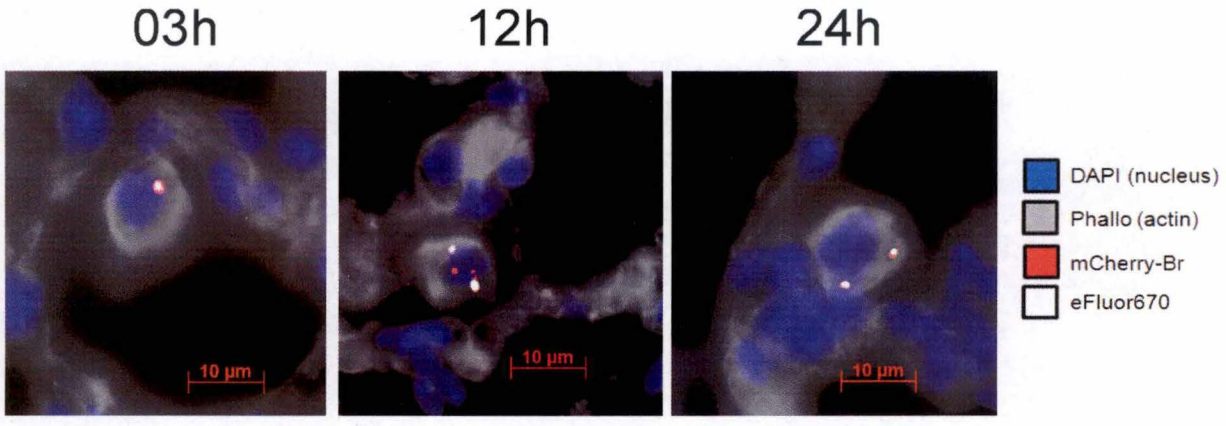

Figure 17: Visualization of *Brucella melitensis* division *in situ* in lungs section, after infection with high dose of eFluor 670-labeled mCherry-expressing *B. melitensis*. At 3 hours post infection, there is a perfect colocalization between the eFluor 670 and Cherry signal, suggesting that these are non-dividing bacteria. At 12 hours post-infection, we can spot eFluor 670-negative mCherry-positive bacteria, suggesting these are daughter cells. At 24 hours, no eFluor-negative are to be found, suggesting that the only bacteria left are non-dividing or mother cells.

II.4.Visualization of *Brucella* division in lungs from infected mice by fluorescence microscopy

The logical follow-up was to test the visualization of *Brucella* growth *in vivo*, by infecting C57BL/6 mice with eFluor 670-labeled mCherry-expressing bacteria, and perform histology analysis on lungs tissues. We infected mice with high doses of labeled bacteria and did histological section of the lungs for fluorescence microscopy analysis.

As expected, we can see that 3 hours after infection, there is still a perfect colocalization of the eFluor 670 and mCherry signal, in highly auto fluorescent fluorescent cells, which appear to be the alveolar macrophages. This suggests that the bacteria did not have the possibility to replicate in the infected cells yet [**Figure 17**]. At 12 hours post infection, we can see that although few bacteria display colocolization between the two signals, lots of them appear eFluor 670 negative and mCherry-positive, suggesting these are newborn bacteria.

Strangely, at 24 hours post infection, we can see the same profile as at 3 hours post infection, as infected cells only contain eFluor 670-labeled mCherry-positive *B. melitensis*. This suggests that the dividing *Brucella* or daughter cells (eFluor 670 negative, mCherry positive) are more targeted or more sensitive to the immune response than the mother cells.

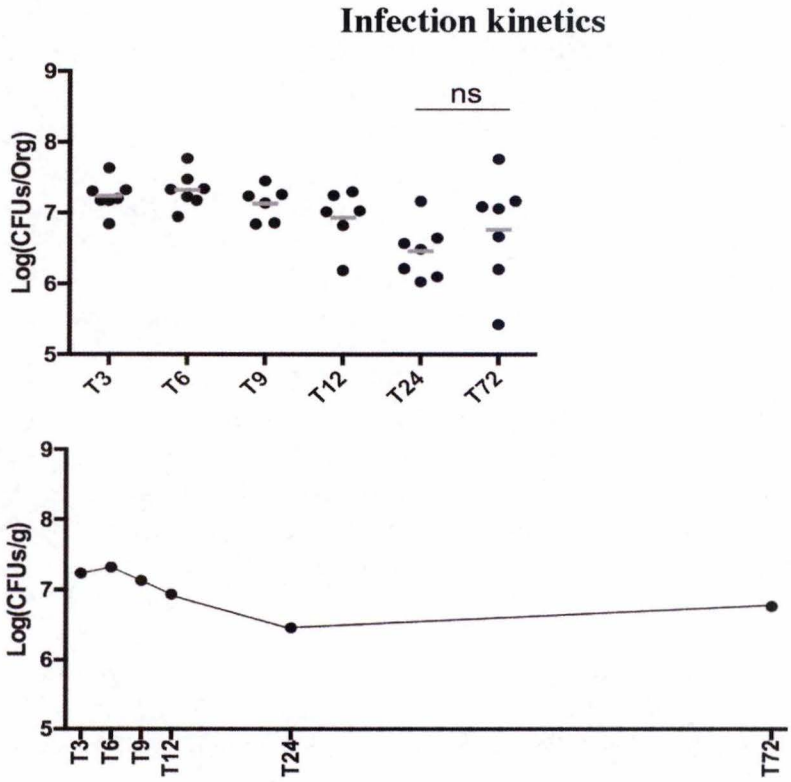

Figure 19: Kinetic approach of the normal course of infection by the mCherry-expressing *Brucella melitensis* following low dose infection in C57BL/6 mice. CFUs have been assessed at times 3 hours, 6 hours, 9 hours, 12 hours, 24 hours and 72 hours after infection.

III. Identification of immune effectors involved in the control of the infection

There are two main hypothesis to explain the fact that, in vivo, the overall number of bacteria per lung is decreasing over time while the number of bacteria per alveolar macrophage is increasing 12 hours after infection [**Figure 17**]. The first one is that *Brucella* is able to grow and replicate in some cells and unable to do so in other, due to the heterogeneity of macrophages (Holt et al. 2008; Hussell & Bell 2014).

The other hypothesis, and in a sense the most logical one, is that the immune system plays a role in the control of infection. This might be the obvious explanation to this phenomenon, but we know that *Brucella* displays lots of strategies to escape not only immune response, but also mere recognition (Lapaque et al. 2006; Barquero-Calvo et al. 2007). Our objective here will be to demonstrate if the immune system does or does not play a role in the control of *Brucella* infection.

III.1. Normal course of infection *in vivo* using mCherry-expressing *Brucella*

As previously shown, there is no impact of the membrane-labeling on the course of infection by *Brucella*. If we assume that it is correct, we will perform the following infections with unlabeled bacteria, since membrane labeling is rather irrelevant for this part and that it will allow us to save time and money to focus on what is essential.

We realized a kinetic approach of the infection *in vivo* as preliminary data. We infected immunocompetent C57BL/6 mice with low doses (2.10^4) of mCherry-expressing *Brucella*, 3, 6, 9, 12, 24 and 72 hours before sacrifice to assess the number of CFUs **[Figure 19]**. As shown by the data, the overall number of CFUs reaches its peak 6 hours post infection before decreasing at 24 hours with a drop of half a Log.

Although non-significant, we can observe a slight increase in the number of CFUs between 24 hours and 72 hours, suggesting that the bacteria which managed to survive are able to strive in the cells.

Let us remind that the increasing number of CFUs between 24 and 72 hours is only a tendency, meaning that the CFUs might decrease until later times before going back up. A more detailed kinetics between 24 hours and 72 hours remains to be done, even though the main point of this Master thesis focuses on the first 24 hours of infection.

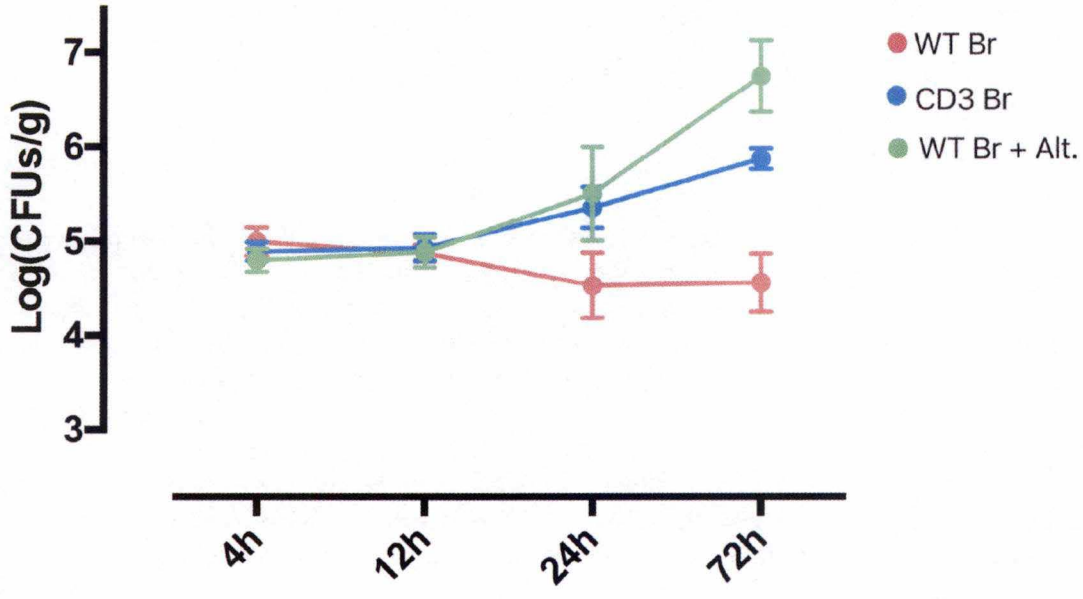

Figure 20: CFUs kinetics of wild type mice (red), CD3-knockout mice (blue) and *Alternaria alternata* sensitized wild type mice (green) infected with low dose of mCherry-expressing *B. melitensis*.

III.2. Impact of asthma and T deficiency in the control of the infection

As discussed in the introduction, if the T_H2 switch induced by allergic asthma is detrimental for the control of infection, we might also wonder what consequences would bring an absence of T_H response. We performed kinetics study with C57BL/6 mice infected with low doses of mCherry-expressing *Brucella*. We used WT immuno competent mice, WT mice sensitized with *Alternaria alternata*, and CD3-deficient mice. The CD3 protein, when associated with the T cell receptor (TCR), allows T cells activation. Therefore, in CD3-deficient mice, there would be no T cell dependent response.

Mice were sacrificed 4, 12, 24 and 72 hours after infection for CFUs counting. Results show that, as previously demonstrated, the CFUs in WT mice are decreasing by approximately half a Log after 24 hours, before slightly increasing at 72 hours **[Figure 20]**.

The CFUs of mice sensitized with *Alternaria alternata* display strong increase of one Log after 24 hours when compared to the WT mice, and approximately two Logs after 72 hours. Surprisingly, the CD3-deficiency seems to display the same tendency than the asthmatic mice but with a less drastic effect. At 24 hours, the CD3-deificient mice display moreless one Log more CFUs than the WT mice.

We can fairly say that the CD3 protein is linked one way or another in the control of the *Brucella* infection. As the CD3 is involved in the immune response, this suggests that the immune system also plays a role in the control of the infection.

III.3. Identification of immune effectors in the control of the infection

We used the same strategy with a set of different immuno-deficient C57BL/6 mice lacking for a protein involved in the detection of the bacteria (TLR2,4,9), the T cells subsets (CD3, TCRαβ, TCRγδ, TAP1, CMH II) or involved in the TH response (TNFR1, IL17RA, IFNγR, IL1R).

As previously shown, in immuno-competent mice, the *Brucella* infection is partially controlled by the immune system, with a drop of half a Log in the number of CFUs between 4 hours and 24 hours after infection, following inoculation of low doses of *Brucella*.

We might argue that if immuno-deficient mice displayed significant decrease in the number of CFUs after 24 hours, similarly to the WT mice, then the infection would be still under control. However, if there is no significant decrease, or against all odds, an increase of the CFUs, then we might conclude that the control of infection is impaired.

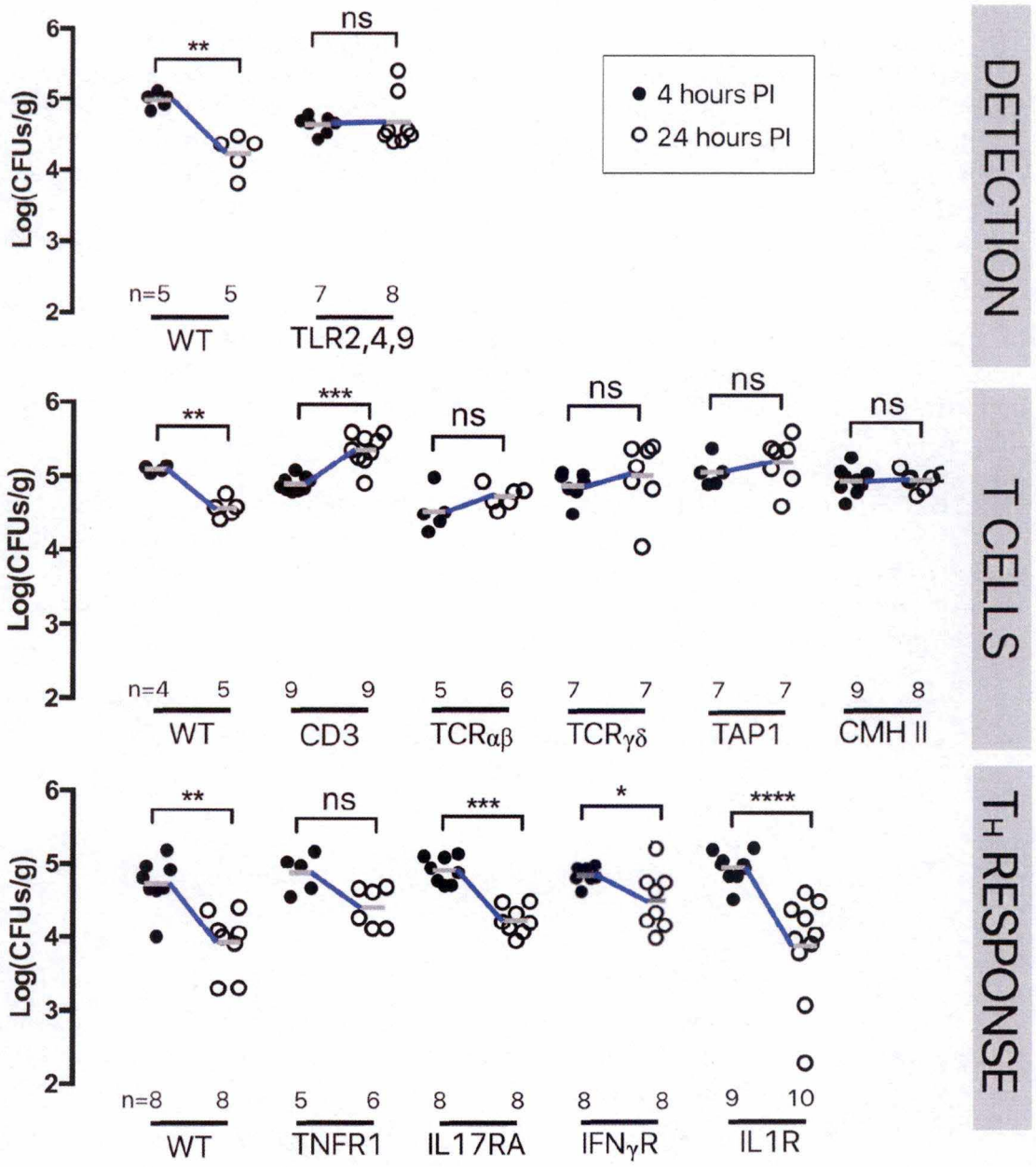

Figure 21 : CFUs analysis of wild type and knockout mice at 4 (full dots) and 24 hours (empty dots) following low dose infection with mCherry-expressing *B. melitensis*. The tendency of the decrease or increase in the number of CFUs (in Log of CFUs per gram of lungs) is represented by a blue line.

We infected mice with low doses of mCherry-expressing *B. melitensis* and collected lungs for CFUs counting 4 hours and 24 hours after infection. Results show various profiles of infection for our different immuno-deficient mice **[Figure 21]**. As expected, the WT groups display a drop of half a Log in the number of CFUs between 4 and 24 hours. If we consider the detection of the bacteria, TLR2,4,9-deficient mice display no significant decrease of the CFUs, meaning that this protein might be involved in the control of the infection.

Surprisingly, all the T cells subsets displayed no significant decrease, but on the contrary, showed an increasing number of CFUs 24 hours after infection. However, the main part of the effectors involved in the T_H response does not seem to be essential in the control of *Brucella* infection.

We also represented the same results in terms of fold decrease **[Figure 22]**, by calculating the ratio between the mean of CFUs at 24 hours and the mean of CFUs at 4 hours. Ratios that are close to 1 would mean that the number of CFUs remains steady and that the control of the infection is impaired. Ratios above the 1 threshold would represent mice displaying an increasing number of CFUs. Finally, ratios significantly lower than 1 would represent mice that are able to control *Brucella* infection.

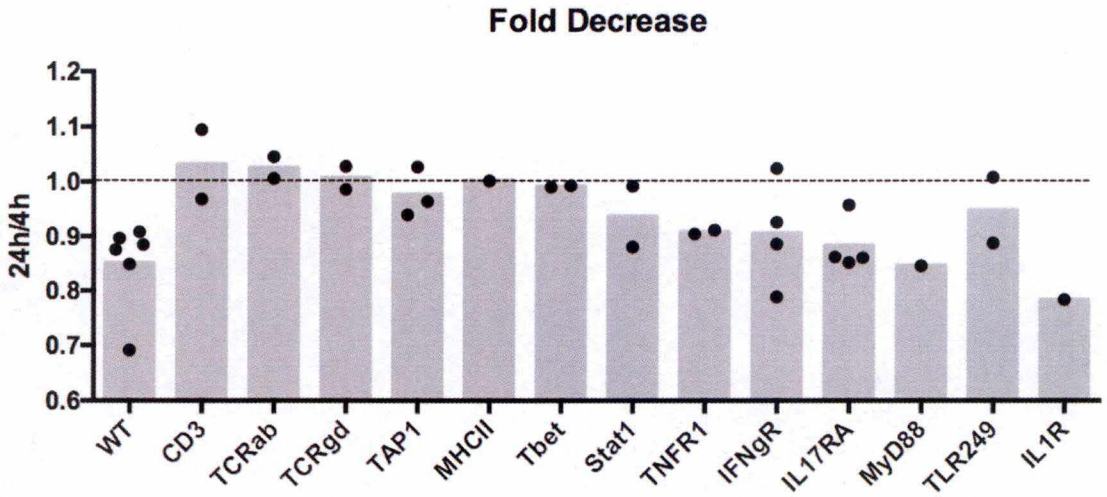

Figure 22: Fold decrease representation of the evolution of CFUs between 4 hours and 24 hours after infection with low dose of mCherry-expressing *B. melitensis*. The ratio is made between the mean Logs of CFUs at 24 hours, and the mean Logs of CFUs at 4 hours. Each dot represents a set of mice sacrificed for the data presented in Figure 21.

Discussion & Perspectives

Brucella spp. are facultative intracellular bacteria displaying unipolar growth and asymmetrical division (Atluri et al. 2011; Brown et al. 2012; Hallez et al. 2004). These bacteria are responsible for brucellosis, a common zoonotic disease that strikes cattle, swine, goats, but also accidently humans (Pappas et al. 2006). *Brucella* spp. are able to perform stealth infection and settle chronically in the organism after colonizing the spleen, sheltered from the immune system (Willey et al. 2011).

Its ability to escape immune detection allows *Brucella* to reach and infect alveolar macrophages where it can grow and replicate before disseminating through the organism (Archambaud et al. 2010). *In vivo* studies led on *Brucella melitensis* infection in mice models showed that, after intranasal infection, *Brucella* is contained in the lungs for the first five days, the lungs being progressively cleared out as the bacteria slowly disseminates to lower organs (von Bargen et al. 2012; Hanot Mambres et al. 2016). The **first objective** of this Master thesis was to confirm the phenotype of the lungs infected cells 24 hours following intranasal infection, by flow cytometry.

The **second objective** of this thesis was to visualize the growth and division of *Brucella melitensis* in the alveolar macrophages *in situ*, by using the unipolar growth particularity of *Brucella* and membrane labeling tools. The unipolar growth feature of *Brucella* has already been manipulated for practical purposes to investigate its pattern of division. Deghelt et al. used the succinimidyl ester membrane labeling, coupled with a fluorochrome (Texas Red) to monitor *Brucella abortus* division, as the labeling protein is anchored in the bacteria peptidoglycan and is not transferred to the daughter cells (Deghelt et al. 2014). This allowed Deghelt to visually differentiate the mother cells from daughter cells.

The **third objective** was to assess the involvement of the immune system in the control of *Brucella* during the first 24 hours of infection by using knockout mice lacking key elements of the immune response. Hanot Mambres et al. demonstrated that five days after intranasal infection, the $CD8^+$ T cells, the $\gamma\delta$ T cells and the IL-17RA are essential for the control of *Brucella* in the lungs (Hanot Mambres et al. 2016). They also showed the role of IFNγ -producing $CD4^+$ T cells, linked to the T_H1 response, in the control of the infection in the spleen (Hanot Mambres et al. 2016).

We also used the induction of allergic asthma in order to trigger a biased T_H2-oriented T_H response as a « T_H1-knockout » model. Potemberg previously used the induction of allergic asthma as a tool to impair the control of *Brucella melitensis* infection by the immune system, leading to an uncontrolled increase of the CFUs in the lungs, after only 24 hours following the infection (Potemberg et al. 2015). The induction of allergic asthma is favoring a one-way T_H2-oriented switch of the T_H response, while the T_H1

response, considered to be the protective response against pathogens like *Brucella*, is inhibited (Barnes 2008; Kasper et al. 2015).

We used C57BL/6 mice, which are predisposed to develop a T_H1 immune reponse (Silva et al. 2011). To investigate the immune response set up against *Brucella* infection, we used C57BL/6 immunocompetent and knockout mice. We performed intranasal infections to follow a more natural route, where *Brucella* would encounter mucosal barrier and immune defenses.

The infected cells following intranasal infection with Brucella melitensis are alveolar macrophages

First we used flow cytometry techniques and a *Brucella* strain expressing a fluorescent protein (mCherry) to quantitatively analyze the phenotype of the infected cells. Archambaud et al. identified these infected cells by fluorescence microscopy as $CD11c^+$, $CD11b^+$, $F4/80^+$ cells with high autofluorescence, and suggested these were alveolar macrophages, after intranasal infection with low doses of *Brucella abortus* (Archambaud et al. 2010). Unable to detect the mCherry-expressing *Brucella melitensis* after 24 hours of infection by flow cytometry, we developed a membrane labeling intense enough to be detectable during the first 48 hours.

We used the eFluor 670, a membrane labeling dye which targets the amines of the outer membrane proteins and emitting in the APC-A channel. The intensity of the signal is barely decreasing after 24 hours, making eFluor 670 a great tool to visualize the infected cells during the early times of infection.

Unfortunately, in order to detect the eFluor 670-labeled mCherry-expressing *Brucella melitensis in vivo* by flow cytometry, we had to use high doses of infection. One might argue that this increasing dose of infection would have consequences, such as the introduction of a new cell target for *Brucella*, thus mimicking the depletion of alveolar macrophages and the apparition of DCs as infected cells (Archambaud et al. 2010).

However, we used a diversified set of antibodies in flow cytometry analyses (data not shown), such as the anti-CD11c, an anti-GR1/Ly6G which is present on the surface of granulocytes (Daley et al. 2007), an anti-F4/80 and an anti-SiglecF both being present on the surface of alveolar macrophages and absent from DCs. These markers combined with the distribution of size (FSC) and granulosity (SSC) lead us to confirm that even with high doses of infection, the infected cells are indeed alveolar macrophages.

For further experiments, it would be interesting to deplete the population of alveolar macrophages using DTR (diphtheria toxin receptor) expressing mice. These mice, initially insensitive to diphtheria toxin, would express the receptor on CD11c-positive

cells such as alveolar macrophages, thus allowing the depletion of these sensitive cells after exposure to the toxin. This would allow us to determine if *Brucella* would be able to perform its infection in absence of those alveolar macrophages by infecting other cell types in the lungs or by extracellular survival before reaching to other organs.

Another perspective would be to use the flow cytometry analysis to sharpen the phenotyping of the infected alveolar macrophages. Indeed, the infection might trigger differences in the expression of effectors inside the macrophage or, if we consider things from another point of view, differences of protein expression might make a cell more susceptible to be infected than another, such as the expression of iNOS/NOS2, or phenotypical differences between alveolar macrophages.

The eFluor 670 membrane labeling allows the distinction between mother and newborn bacteria

We also took advantage of the eFluor 670 labeling dye to differentiate mother from daughter bacteria by fluorescence microscopy, as the eFluor 670 label is only preserved by mother cells.

The flow cytometry data showed no significant differences in the intensity of both eFluor 670 and mCherry signal between 4 and 24 hours post infection in alveolar macrophages, while the mCherry signal was increasing at 48 hours after infection, suggesting that the bacteria successfully replicated in the alveolar macrophages between 24 and 48 hours after infection. Interestingly, this also suggests that the number of *Brucella* per cell does not increase during the first 24 hours, and even more, due to the slight decrease of eFluor 670-positive cells at 24 hours, that the infection is partially counteracted.

One could spot an odd signal both in the eFluor 670/APC-A and mCherry/Texas Red-A channels in naïve mice, or out of the gate displayed on the plot. Why would there be a positive signal in alveolar macrophages of non-infected naïve mice? This observed background signal might be explained, for example, by the presence of molecules containing aromatic cycles like flavins or NADH (Piston et al. 1995) and does not imply that mCherry or eFluor 670 proteins are found in the naïve mice. We can also argue that the small positive signal detected, and which is mostly concentrated in the alveolar macrophages gate, is due to macrophages auto fluorescence.

We performed *in vitro* investigations of *Brucella melitensis* growth and division by labeling liquid cultures of mCherry-expressing *Brucella* with the eFluor 670. Over time, we could make the difference between mother and newborn cells as the amount of eFluor 670 transferred to daughter cells was statistically lower and lower after division. These results suggested that even in mild quantities, the eFluor 670 label was transferred to daughter cells, probably through the growing pole.

In vivo studies of *Brucella melitensis* division presented additional results with fluorescence microscopy analysis. Indeed, these results showed that *Brucella* was able to proliferate between 3 and 12 hours in alveolar macrophages, due to the presence of unlabeled daughter cells. However, the presence of only labeled bacteria at 24 hours post infection leads to the hypothesis that by proliferating, *Brucella* triggers the immune response, whether of the alveolar macrophage itself or other immune cells such as the NK cells. Thus, the only bacteria that survive are wether non-dividing *Brucella* that did not replicate in the first place, or mother cells that would be somehow more resistant than daughter cells. Interestingly, this observation matches with the flow cytometry analysis, as both eFluor 670 and mCherry signals display little variation. However, as both protocols use the same infection doses of bacteria, this *Brucella* recognition and elimination might be an artifact due to these particularly high doses, easily triggering the immune response.

The flow cytometry analysis might offer great possibilities regarding the differences between the alveolar macrophages. We could think that some alveolar macrophages are not susceptible for *Brucella* entry of replication, or that some are able to kill *Brucella* after division, or that some macrophages are unable to control the infection at all. We could take advantage of cell sorting techniques to separate *Brucella*-infected and non-infected macrophages and compare disparities in genes expression between these cells. We also might argue that if the leftover bacteria at 24 hours are not non-dividing cells but resistant mother cells, then we could also spot differences in gene expression between daughter and mother cells.

Variations in gene expression might be investigated by transposon sequencing to compare the expression in *Brucella* whether they grow in liquid culture, or in infection *in vitro* (in RAW 264.7 macrophages) or *in vivo* in mice. Then again, we could spot variations *in vivo* whether the targeted cells are alveolar macrophages or, subsequently to the depletion of $CD11c^+$ cells, other cell types.

Another interesting perspective would be to assess the cell to cell spreading, enlightened by Starr and its studies on the roles of aBCV (Starr et al. 2012). One could create a strain of *Brucella melitensis* expressing a fluorescent protein emitting in the APC-A channel (to avoid the risk of interference with the alveolar macrophages autofluorescence), such as the Azurite fluorescent protein (Mena et al. 2006) or the CFP (Malkani & Schmid 2011) as long as those protein are resistant to fixation with paraformaldehyde. This strain would allow co-infection in mice with the mCherry-expressing *Brucella* at specific intermediary dose allowing in one hand the detection of the bacteria and in the other hand an infection involving one bacteria per alveolar macrophages. This would allow us, after *Brucella* division, to assess cell to cell spreading by quantifying the number of GFP-positive bacteria in an infected cells already containing a majority of mCherry-positive bacteria, or vice versa.

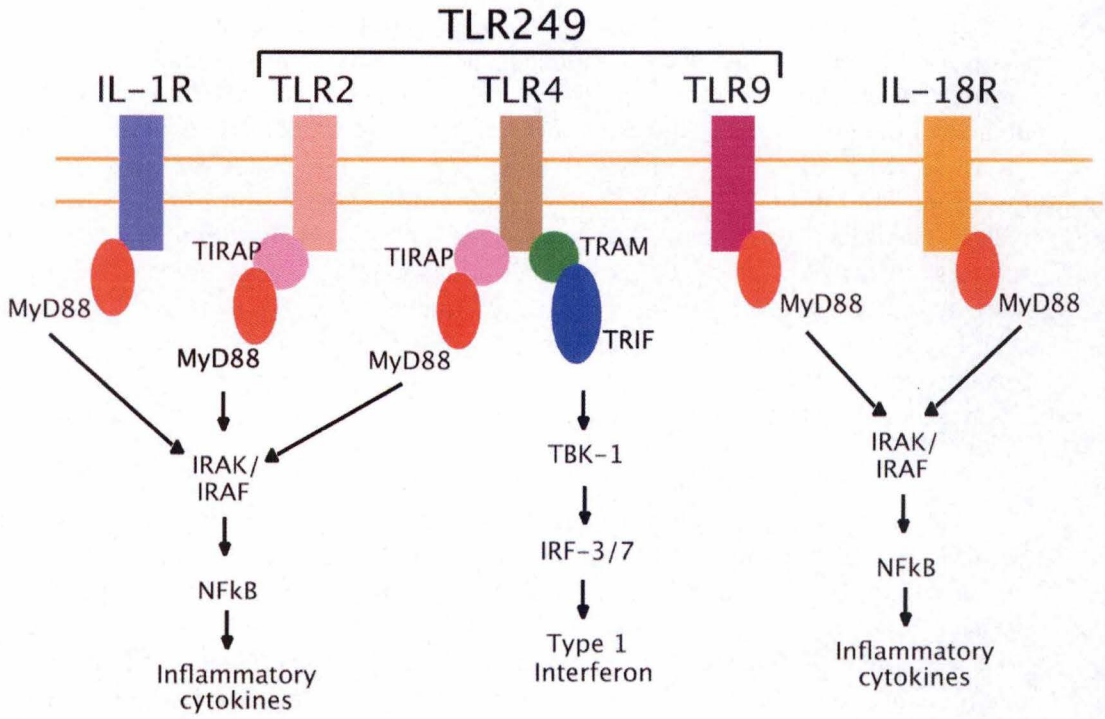

Figure 23 : TLR 2,4,9, IL-1R and IL-18R signalling pathways.

Key effectors of the immune system play a role in the control of Brucella melitensis during the first 24 hours of infection

We used several knockout mice to perform CFUs analysis and spot effectors of the immune response that might be involved in the control of *Brucella*, 24 hours after intranasal infection. We also used the induction of allergic asthma in the same fashion than Potemberg as a "T_H2 biaised / T_H1-knockout" model (Potemberg et al. 2015). Results showed that, although lower, the absence of CD3 (thus preventing T cell dependent response) seems to have the same impacts on the CFUs than the induction of allergic asthma, namely an increase of these CFUs, suggesting a lack of control of the infection.

The impact of allergic asthma on the control of the *Brucella* infection seems to be dependent of T_H2-related IL-10, IL-4/STAT6 signaling pathway and regulatory $CD4^+$ T cells (source of IL-10) (Machelart et al. n.d.; Couper et al. 2008). Indeed, the T_H2 response has been correlated with an overall immunosuppressive response mediated by TGFβ and IL-10, inhibiting the T_H1 response (Huang et al. 2014; Robinson 2009) and the activity of NK cells and macrophages by downregulating MHC II expression and proinflammatory cytokines such as IL-1 and TNFα (Couper et al. 2008). This response is initially settled to inhibits the IgE production, thus soothing the allergic phenotype, but also favoring *Brucella* persistence in mice by reducing the effector functions of infected macrophages (Xavier, Winter, Spees, Nguyen, et al. 2013).

We also used several mice deficient for proteins involved in the detection of the bacteria, the T cells subsets and the development of the T_H response. Our results showed that during the first 24 hours, the TLR 2,4,9, playing a role on the detection of the bacteria, is involved in the control of the infection.

To investigate further the signaling cascade following the recognition of *Brucella* by the Toll-like receptors, we performed CFUs analysis of MyD88-knockout mice (data not shown). However, this preliminary investigation remains to be repeated, as well as other adaptor proteins that might be involved in the TLR recognition pathways [**Figure 23**].

All the T cells subsets used during this thesis seems to be involved as well, namely the CD3, the TCRαβ, the TCRγδ, the TAP1 (which induce an absence of CMH I proteins) and the CMH II proteins. However, proteins involved in the development of the T_H response (TNFR1, IL17RA, IFNγR, IL-1R) does not appear to be essential during the first 24 hours. These surprising results suggest a role of T cells even during the first 24 hours of infection, even though the development of a T_H response does not seem to be essential.

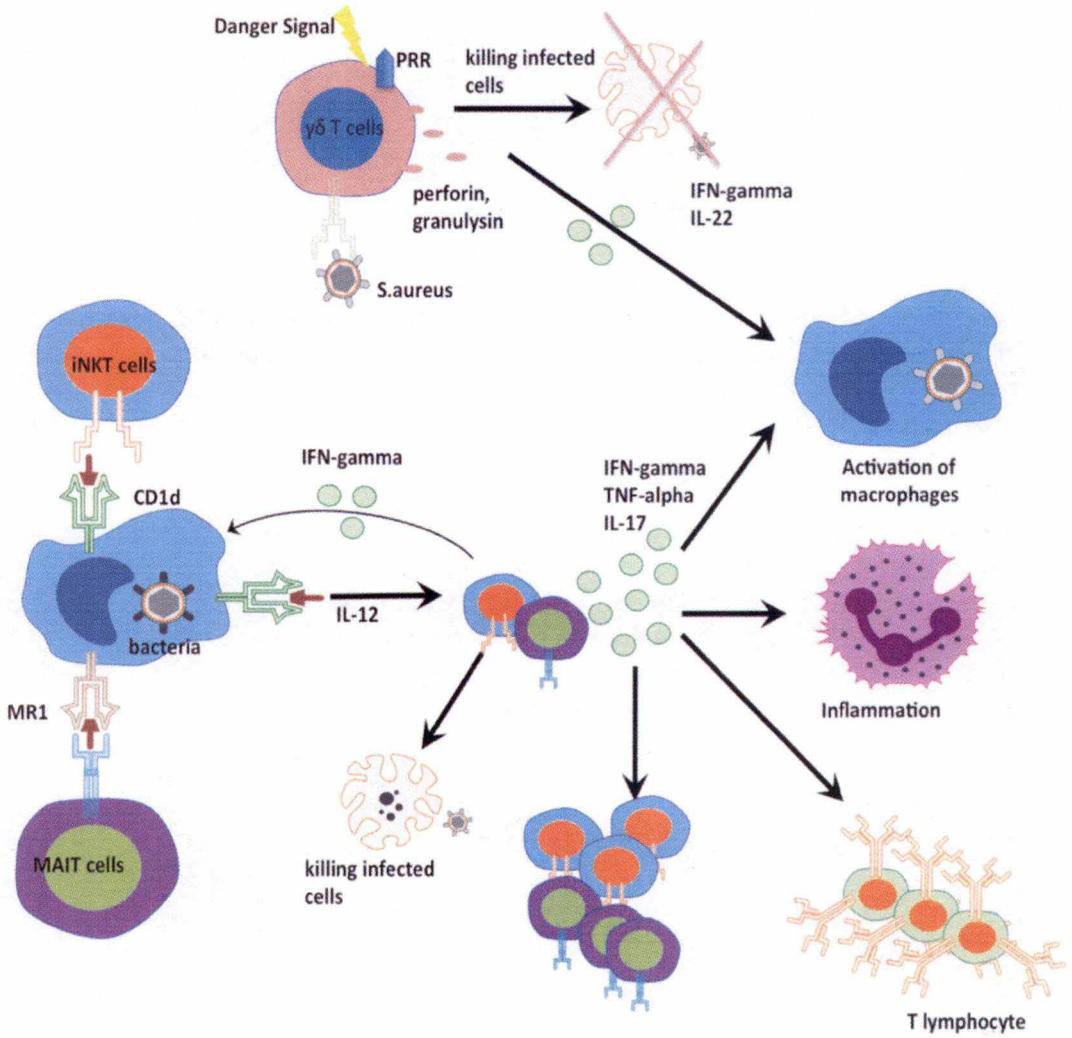

Figure 24: Roles of unconventional T cells (iNKT, MAIT and γδ T cells) in the early times of anti-microbial immunity (Haeryfar & Mallevaey 2016).

Strangely, Hanot Mambres results showed that after five days, the $CD8^+$ T cells and the γδ T cells were relevant for the control of infection, concording with our findings (Hanot Mambres et al. 2016). However, she spotted IL-17RA as essential for *Brucella* control at five days post infection, even though this seems not to be the case after 24 hours of infection.

The involvement of T cells in early times of infection might be puzzling, as $CD4^+$ and $CD8^+$ have always been linked to recognition of pathogen peptides through MHC molecules, which suggests a more delayed immune response. However, recent studies enlightened unconventional innate-like T cells which do not require MHC molecules and act as an emergency response (less than two hours) to infection and act as a bridge between innate and adaptive response (Haeryfar & Mallevaey 2016). These unconventional T cells are an heterogeneous group of γδ innate T cells, and αβ innate T cells which include CD1-restricted NK T cells, which recognize lipid antigens, and MR1-restricted mucosa-associated invariant T cells (MAIT) which recognize bacteria-derived metabolites (Haeryfar & Mallevaey 2016; Howson et al. 2015). Their role, *inter alia*, is to secrete T_H1-, T_H2- and T_H17-derived cytokines in the early times of infection to modulate the functions of immunity related cells (Haeryfar & Mallevaey 2016).

Invariant NK T cells (iNKT) express the TCR with invariant α chain (Kasper et al. 2015; Haeryfar & Mallevaey 2016) and constitute the first line in emergency responses against pathogens, as they accumulate at the site of infection to activate other immune cells, for example through the production of IFNγ (Haeryfar & Mallevaey 2016; Slauenwhite & Johnston 2015) [**Figure 24**]. GRAM negative bacteria such as *Brucella* can also directly activate iNKT cells through the glycosphingolipids present in the cell wall (Haeryfar & Mallevaey 2016).

MAIT cells also express an invariant TCRα chain and are predominant in mucosal tissues (Napier et al. 2015). They are able to secrete inflammatory cytokines and perform cytotoxicity activites through the exocytosis of perforin and granzymes (Howson et al. 2015; Napier et al. 2015). iNKT cells, MAIT cells and γδ T cells express the same C-type lectin molecule CD161 (Haeryfar & Mallevaey 2016). We might imagine the use $CD161^+$ knockout mice, or antibodies driven against the $CD161^+$ proteins, to investigate further the role of those innate-like T cells.

Bibliography

Akira, S. & Kiyoshi, T., 2004. Toll-like receptor signalling. *Nature reviews. Immunology*, 4(July).

Archambaud, C. et al., 2010. Contrasting roles of macrophages and dendritic cells in controlling initial pulmonary Brucella infection. *European Journal of Immunology*, 40(12), pp.3458–3471.

Ariza, J. et al., 2007. Perspectives for the treatment of brucellosis in the 21st century: The Ioannina recommendations. *PLoS Medicine*, 4(12), pp.1872–1878.

Atluri, V.L. et al., 2011. Interactions of the Human Pathogenic Brucella Species with Their Hosts. *Annual Review of Microbiology*, 65(1), pp.523–541. Available at: http://dx.doi.org/10.1146/annurev-micro-090110-102905.

von Bargen, K., Gorvel, J.P. & Salcedo, S.P., 2012. Internal affairs: Investigating the Brucella intracellular lifestyle. *FEMS Microbiology Reviews*, 36(3), pp.533–562.

Barnes, P.J., 2008. Review series The cytokine network in asthma and chronic obstructive pulmonary disease. *The Journal of clinical investigation*, 118(11), pp.3546–3556.

Barquero-Calvo, E. et al., 2007. Brucella abortus uses a stealthy strategy to avoid activation of the innate immune system during the onset of infection. *PLoS ONE*, 2(7).

Biswas, S.K. & Mantovani, A., 2012. Orchestration of metabolism by macrophages. *Cell Metabolism*, 15(4), pp.432–437. Available at: http://dx.doi.org/10.1016/j.cmet.2011.11.013.

Boschiroli, M.L. et al., 2002. The Brucella suis virB operon is induced intracellularly in macrophages. *PNAS*, 99(3), pp.1544–1549.

Brogden, K.A. et al., 2003. Antimicrobial peptides in animals and their role in host defences. *International Journal of Antimicrobial Agents*, 22(5), pp.465–478.

Brown, P.J.B. et al., 2012. Polar growth in the Alphaproteobacterial order Rhizobiales. *Proceedings of the National Academy of Sciences*, 109(8), pp.3190–3190.

Castañeda-Roldán, E.I. et al., 2006. Characterization of SP41, a surface protein of Brucella associated with adherence and invasion of host epithelial cells. *Cellular Microbiology*, 8(12), pp.1877–1887.

Celli, J. et al., 2003. Brucella evades macrophage killing via VirB-dependent sustained interactions with the endoplasmic reticulum. *The Journal of experimental medicine*, 198(4), pp.545–556.

Celli, J., 2015. The changing nature of the Brucella-containing vacuole. *Cellular Microbiology*, 17(May), pp.951–958.

Chen, F. et al., 2012. An essential role for the Th2-type response in limiting tissue damage during helmit infection. *National Institute of Health*, 18(2), pp.260–266.

Comerci, D.J. et al., 2001. Essential role of the virB machinery in the maturation of the Brucella abortus-containing vacuole. *Cellular Microbiology*, 3(3), pp.159–168.

Copin, R. et al., 2012. In situ microscopy analysis reveals local innate immune response developed around Brucella infected cells in resistant and susceptible mice. *PLoS Pathogens*, 8(3).

Corbel, M., 1997. Brucellosis : an Overview. , 3(2), pp.213–221.

Couper, K., Blount, D. & Riley, E., 2008. IL-10: the master regulator of immunity to infection. *Journal of immunology*, 180(9), pp.5771–5777.

Daley, J.M. et al., 2007. Use of Ly6G-specific monoclonal antibody to deplete neutrophils in mice.

Deghelt, M. et al., 2014. G1-arrested newborn cells are the predominant infectious form of the pathogen Brucella abortus. *Nature communications*, 5, p.4366. Available at: http://www.ncbi.nlm.nih.gov/pubmed/25006695.

Delrue, R.M. et al., 2001. Identification of Brucella spp. genes involved in intracellular trafficking. *Cellular Microbiology*, 3(7), pp.487–497.

Felix, C. et al., 2014. The Brucella TIR domain containing proteins BtpA and BtpB have a structural WxxxE motif important for protection against microtubule depolymerisation. , pp.1–15.

Godfroid, J. et al., 2011. Brucellosis at the animal / ecosystem / human interface at the beginning of the 21st century. *Preventive Veterinary Medicine*, 102(2), pp.118–131. Available at: http://dx.doi.org/10.1016/j.prevetmed.2011.04.007.

Grubor, B., Meyerholz, D. & Ackermann, M., 2006. Collectins and cationic antimicrobial peptides of the respiratory epithelia. , 100(2), pp.130–134.

Haagsman, H.P., 2002. Structural and functional aspects of the collectin SP-A. *Immunobiology*, 205(4–5), pp.476–89. Available at: http://www.ncbi.nlm.nih.gov/pubmed/12396009.

Habibzay, M., Weiss, G. & Hussell, T., 2013. Bacterial superinfection following lung inflammatory disorders. *Future microbiology*, 8(2), pp.247–56. Available at: http://www.ncbi.nlm.nih.gov/pubmed/23374129.

Haeryfar, S.M.M. & Mallevaey, T., 2016. Cd1- and mr1-restricted t cells in antimicrobial immunity

Hallez, R. et al., 2004. Morphological and functional asymmetry in alpha-proteobacteria. *Trends in microbiology*, 12(8), pp.361–365.

Hanot Mambres, D. et al., 2016. Identification of Immune Effectors Essential to the Control of Primary and Secondary Intranasal Infection with Brucella melitensis in Mice. *The Journal of Immunology*, 196(9), pp.3780–3793. Available at: http://www.jimmunol.org/cgi/doi/10.4049/jimmunol.1502265.

Hanot Mambres, D. et al., 2015. In situ characterization of splenic brucella melitensis reservoir cells during the chronic phase of infection in susceptible mice. *PLoS ONE*, 10(9), pp.1–20.

Hoefel, D. et al., 2003. A comparative study of carboxyfluorescein diacetate and carboxyfluorescein diacetate succinimidyl ester as indicators of bacterial activity. *Journal of Microbiological Methods*, 52(3), pp.379–388.

Hoffmann, J. a et al., 1999. Phylogenetic perspectives in innate immunity. *Science (New York, N.Y.)*, 284(5418), pp.1313–1318.

Holmskov, U., Thiel, S. & Jensenius, J.C., 2003. Collectins and ficolins : Humoral Lectins of the Innate Immune Defense. *Annual Review of Immunology*, 21(1), pp.547–578. Available at: http://www.annualreviews.org/doi/abs/10.1146/annurev.immunol.21.120601.140954.

Holt, P.G. et al., 2008. Regulation of immunological homeostasis in the respiratory tract. *Nature reviews. Immunology*, 8(2), pp.142–152.

Howson, L.J., Salio, M. & Cerundolo, V., 2015. MR1-restricted mucosal-associated invariant T cells and their activation during infectious diseases. *Frontiers in Immunology*, 6(JUN).

Huang, L. et al., 2014. Eosinophil-derived IL-10 supports chronic nematode infection. *Journal of immunology (Baltimore, Md. : 1950)*, 193(8), pp.4178–87. Available at: http://www.pubmedcentral.nih.gov/articlerender.fcgi?artid=4241261&tool=pmcentrez&rendertype=abstract.

Hussell, T. & Bell, T.J., 2014. Alveolar macrophages: plasticity in a tissue-specific context. *Nature Reviews Immunology*, 14(2), pp.81–93. Available at: http://www.nature.com/doifinder/10.1038/nri3600.

Kasper, D. et al., 2015. Harrison's Principles of Internal Medicine. , 19th Editi.

Kaufmann, S.H.E., 2007. The contribution of immunology to the rational design of novel antibacterial vaccines. *Nature reviews. Microbiology*, 5(7), pp.491–504. Available at: http://www.ncbi.nlm.nih.gov/pubmed/17558425.

Ke, Y. et al., 2015. Type IV secretion system of Brucella spp. and its effectors. *Frontiers in cellular and infection microbiology*, 5(October), p.72. Available at: http://www.pubmedcentral.nih.gov/articlerender.fcgi?artid=4602199&tool=pmcentrez&rendertype=abstract.

Ko, J. et al., 2002. Virulence criteria for Brucella abortus strains as determined by interferon regulatory factor 1-deficient mice. *Infection and Immunity*, 70(12), pp.7004–7012.

Lapaque, N. et al., 2006. Differential inductions of TNF-α and IGTP, IIGP by structurally diverse classic and non-classic lipopolysaccharides. *Cellular Microbiology*, 8(3), pp.401–413.

Lazarevic, V. & Glimcher, L.H., 2011. T-bet in disease. *Nature Immunology*, 12(7), pp.597–606. Available at: http://www.nature.com/doifinder/10.1038/ni.2059.

Liew, F.Y., 2012. IL-33: a Janus cytokine: Table 1. *Annals of the Rheumatic Diseases*, 71(Suppl 2), pp.i101–i104. Available at: http://ard.bmj.com/lookup/doi/10.1136/annrheumdis-2011-200589.

Machelart, Arnaud; Potemberg, Georges; Lagneaux, M. et al., (Unpublished) Allergic asthma favor Brucella growth and persistence in lung via IL-10 dependent pathways.

Machelart, A., 2016. Impact de l 'asthme allergique et de l ' infection par Trypanosoma brucei sur le contrôle de l 'infection par Brucella melitensis chez la souris.

Malkani, N. & Schmid, J.A., 2011. Some secrets of fluorescent proteins: Distinct bleaching in various mounting fluids and photoactivation of cyan fluorescent proteins at YFP-excitation. *PLoS ONE*, 6(4), pp.1–7.

Marichal, T. et al., 2010. Interferon response factor 3 is essential for house dust mite-induced airway allergy. *Journal of Allergy and Clinical Immunology*, 126(4).

Mena, M. a et al., 2006. Blue fluorescent proteins with enhanced brightness and photostability from a structurally targeted library. *Nature biotechnology*, 24(12), pp.1569–1571.

Merckx, M. et al., 2016. Master Thesis: Analysis of Brucella melitensis cell cycle in lungs alveolar macrophages in vivo.

Moreno, E., 2014. Retrospective and prospective perspectives on zoonotic brucellosis. , 5(May), pp.1–18.

Muraille, E., Leo, O. & Moser, M., 2014. Th1/Th2 paradigm extended: Macrophage polarization as an unappreciated pathogen-driven escape mechanism? *Frontiers in Immunology*, 5(NOV), pp.1–12.

Murphy, E.A. et al., 2001. Interferon-γ is crucial for surviving a Brucella abortus infection in both resistant C57BL/6 and susceptible BALB/c mice. *Immunology*, 103(4), pp.511–518.

Napier, R.J. et al., 2015. The role of mucosal associated invariant T cells in antimicrobial immunity. *Frontiers in Immunology*, 6(JUN), pp.1–10.

O'Neill, L.A.J., Golenbock, D. & Bowie, A.G., 2013. The history of Toll-like receptors - redefining innate immunity. *Nature reviews. Immunology*, 13(6), pp.453–60. Available at: http://dx.doi.org/10.1038/nri3446.

Odegaard, J.I. & Chawla, A., 2012. Alternative Macrophage Activation and Metabolism. , pp.275–297.

Oliveira, S.C., Giambartolomei, G.H. & Cassataro, J., 2011. Confronting the barriers to develop novel vaccines against brucellosis. *Expert Rev Vaccines*, 10(9), pp.1291–1305. Available at: http://www.ncbi.nlm.nih.gov/pubmed/21919619.

Ouyang, W., Kolls, J. & Zheng, Y., 2012. The biological functions of Th17 cell effector cytokines in inflammation. *Immunity*, 28(4), pp.454–467.

Palm, N., Rosenstein, R. & Medzhitov, R., 2012. Allergic Host Defenses. *Nature*, 484(2), pp.130–134.

Pappas, G. et al., 2006. The new global map of human brucellosis. *The Lancet infectious diseases*, 6(2), pp.91–99.

Peng, M.Y. et al., 2008. Interleukin 17-producing gamma delta T cells increased in patients with active pulmonary tuberculosis. *Cellular & molecular immunology*, 5(3), pp.203–208.

Piston, D.W., Masters, B.R. & Webb, W.W., 1995. Three-dimensionally resolved NAD(P)H cellular metabolic redox imaging of the in situ cornea with two-photon excitation laser scanning microscopy. *Journal of microscopy*, 178(Pt 1), pp.20–27. Available at: http://www.ncbi.nlm.nih.gov/pubmed/7745599.

Potemberg, G. et al., 2015. Master Thesis: The influence of asthma on the mouse ability to control the intranasal infection by the bacteria Brucella melitensis. , pp.1–110.

Robinson, D.S., 2009. Regulatory T cells and asthma. *Clinical and Experimental Allergy*, 39(9), pp.1314–1323.

Salcedo, S.P. et al., 2008. Brucella control of dendritic cell maturation is dependent on the TIR-containing protein Btp1. *PLoS Pathogens*, 4(2).

Seleem, M.N., Boyle, S.M. & Sriranganathan, N., 2010. Brucellosis : A re-emerging zoonosis. , 140, pp.392–398.

Sengupta, D. et al., 2010. Subversion of innate immune responses by Brucella through the targeted degradation of the TLR signaling adapter, MAL. *Journal of immunology (Baltimore, Md. : 1950)*, 184(2), pp.956–64. Available at: http://www.pubmedcentral.nih.gov/articlerender.fcgi?artid=3644118&tool=pmcentrez&rendertype=abstract.

Sieira, R. et al., 2000. A Homologue of an Operon Required for DNA Transfer in. *Society*, 182(17), pp.4849–4855.

Silva, T.M.A. et al., 2011. Laboratory animal models for brucellosis research. *Journal of Biomedicine and Biotechnology*, 2011.

Slauenwhite, D. & Johnston, B., 2015. Regulation of NKT cell localization in homeostasis and infection. *Frontiers in Immunology*, 6(MAY).

Starr, T. et al., 2008. Brucella intracellular replication requires trafficking through the late endosomal/lysosomal compartment. *Traffic*, 9(5), pp.678–694.

Starr, T. et al., 2012. Selective subversion of autophagy complexes facilitates completion of the Brucella intracellular cycle. *Cell Host and Microbe*, 11(1), pp.33–45.

Swain, S.L., Mckinstry, K.K. & Strutt, T.M., 2012. Expanding roles for CD4+ T cells in immunity to viruses. *Nat. Rev. Immunology*, 12(2), pp.136–148.

Vantourout, P. & Hayday, A., 2013. Six-of-the-best: unique contributions of γδ T cells to immunology. *Nature Reviews Immunology*, 13(2), pp.88–100. Available at: http://www.pubmedcentral.nih.gov/articlerender.fcgi?artid=3951794&tool=pmcentrez&rendertype=abstract.

Vermaelen, K. & Pauwels, R., 2004. Accurate and simple discrimination of mouse pulmonary dendritic cell and macrophage populations by flow cytometry: Methodology and new insights. *Cytometry Part A*, 61(2), pp.170–177.

Vitry, M.A. et al., 2014. Brucella melitensis invades murine erythrocytes during infection. *Infection and Immunity*, 82(9), pp.3927–3938.

Willey, J.M., Sherwood, L.M. & Christopher, J., 2011. Prescott's Microbiology. , 8th Editio(1), pp.64–65.

William, E., 2013. *Fundamental Immunology* 7th Editio., Lippincott Williams & Wilkins.

Williams, A., 2012. *Immunology: Mucosal and body surface defenses*, Wiley-Blackwell.

Wright, J.R., 2004. Host defense functions of pulmonary surfactant. *Biology of the Neonate*, 85(4), pp.326–332.

Xavier, M.N., Winter, M.G., Spees, A.M., Nguyen, K., et al., 2013. CD4+ T Cell-derived IL-10 Promotes Brucella abortus Persistence via Modulation of Macrophage Function. *PLoS Pathogens*, 9(6).

Xavier, M.N., Winter, M.G., Spees, A.M., Den Hartigh, A.B., et al., 2013. PPARγ - mediated increase in glucose availability sustains chronic brucella abortus infection in alternatively activated macrophages. *Cell Host and Microbe*, 14(2), pp.159–170.

Zabriskie, J.B., 2009. *Essential Clinical Immunology*, Cambridge University Press.

J. JONET - *Secrétariat*
Dépt. BIOLOGIE F.U.N.D.P.
Rue de Bruxelles 61
B-5000 NAMUR (Belgique)
Tél. +32(0)81.72.44.18
Fax +32(0)81.72.44.20